Informing shigellosis prevention and control through pathogen genomics

Authors:

Rebecca J. Bengtsson[1], Adam J. Simpkin[2], Caisey V. Pulford[1,7], Ross Low[3], David A. Rasko[5], Daniel J. Rigden[2], Neil Hall[3,4], Eileen M. Barry[6], Sharon M. Tennant[6], Kate S. Baker[1]

Affiliations:

[1] Clinical Infection, Microbiology and Immunity, Institute of Infection, Veterinary and Ecological Sciences, The University of Liverpool, UK

[2] Biochemistry and Systems Biology, Institute of Systems, Molecular and Systems Biology, The University of Liverpool, UK

[3] Earlham Institute, Norwich Research Park, Norwich, UK

[4] School of Biological Sciences, University of East Anglia, Norwich, UK

[5] Department of Microbiology and Immunology, Institute for Genome Sciences, University of Maryland School of Medicine, Baltimore, Maryland, USA

[6] Center for Vaccine Development and Global Health, University of Maryland School of Medicine, Baltimore, Maryland, USA

[7] Blood Safety, Hepatitis, Sexually Transmitted Infections and HIV Service, National Infection Service, Public Health England, London, UK

Corresponding Author:

Kate S. Baker

Email: kbaker@liverpool.ac.uk

Abstract

Shigella spp. are the leading bacterial cause of severe childhood diarrhoea in low- and middle- income countries (LMIC), are increasingly antimicrobial resistant and have no licensed vaccine. We performed genomic analyses of 1246 systematically collected shigellae from seven LMIC to inform control and identify factors that could limit the effectiveness of current approaches. We found that *S. sonnei* contributes ≥20-fold more disease than other *Shigella* species relative to its genomic diversity and highlight existing diversity and adaptative capacity among *S. flexneri* that may generate vaccine escape variants in <6 months. Furthermore, we show convergent evolution of resistance against the current recommended antimicrobial among shigellae. This demonstrates the urgent need to integrate existing genomic diversity into vaccine and treatment plans for *Shigella*, and other pathogens.

Introduction

Shigellosis is a diarrhoeal disease responsible for approximately 212,000 annual deaths and accounting for 13.2% of all diarrhoeal deaths globally (1). The Global Enteric Multicenter Study (GEMS) was a large case-control study conducted between 2007 and 2011, investigating the aetiology and burden of moderate-to-severe diarrhoea (MSD) in children less than five years old in low- and middle-income countries (LMICs) (2). GEMS revealed shigellosis as the leading bacterial cause of diarrhoeal illness in children, who represent a major target group for vaccination (3). The aetiological agents are *Shigella*, a Gram-negative genus comprised of *S. flexneri*, *S. sonnei*, *S. boydii* and *S. dysenteriae*, with the former two serotypes causing the majority (90%) of attributable shigellosis in children in LMICs (3). Currently, the disease is primarily managed through supportive care and antimicrobial therapy. However, there has been an increase in antimicrobial resistance (AMR) among *Shigella* (4). Particularly concerning is the rise of resistance against the fluoroquinolone antimicrobial ciprofloxacin, the current World Health Organisation (WHO) recommended treatment, such that fluoroquinolone-resistant (FQR) *Shigella* is one of a dozen pathogens for which WHO notes new antimicrobial therapies are urgently needed (5). The high disease burden and increasing AMR of *Shigella* call for improvements in treatment and management options for shigellosis, and significant momentum has built to rise to this challenge.

However, there is still no licenced vaccine available for *Shigella* and one of the main challenges in its development is the considerable genomic and phenotypic diversity of the organisms (6). The distinct lipopolysaccharide O-antigen structures of *Shigella* determine its serotype and is responsible for conferring the short to medium term serotype-specific immunity following infection (7-10). Hence, considerable efforts are focused on generating O-antigen specific vaccines. However, with the exception of the single serotype *S. sonnei*, each species encompasses multiple diverse serotypes: 14 serotypes/subserotypes for *S. flexneri*, 19 for *S. boydii* and 15 for *S. dysenteriae* (11). Thus, for serotype-targeted vaccine approaches, multivalent vaccines are proposed to provide broad protection against disease (6, 12). Furthermore, while O-antigen conjugates are a leading strategy, challenge studies have recently demonstrated poor efficacy (13, 14). An attractive alternative and/or complement to serotype-targeted vaccine formulations are specific subunit vaccines which target highly conserved proteins and may offer broad protection. There are several candidates in development that have demonstrated protection in animal models (15, 16), but the degree of antigenic variation for these targets among the global *Shigella* population remains unknown.

Whole-genome sequencing analysis (WGSA) provides sufficient discriminatory power to resolve phylogenetic relationships and characterise diversity of bacterial pathogens, essential to informing vaccine development and other aspects of disease control (17, 18). However, these critical analysis tools are yet to be applied to a pathogen collection appropriate for broadly informing shigellosis control in the critical demographic of children in LMICs. Here, we apply WGSA to *Shigella* isolates sampled during GEMS, representing 1,246 systematically collected isolates from across seven nations in sub-Saharan Africa and South Asia with some of the highest childhood mortality rates (2, 19). We found evidence of the potential benefit of genomic subtype-based targeting, characterised pathogen features that will complicate current vaccine approaches, and highlighted regional differences among *Shigella* diversity, as well as determinants of AMR, including convergent evolution toward resistance against currently recommended treatments. Our analysis of this unparalleled pathogen collection informs the control and prevention of shigellosis in those populations most vulnerable to disease.

Results and Discussion

Regional diversity of Shigella spp. across LIMC

To date, this is the largest representative dataset of *Shigella* genomes from LMICs (*n*=1246), collected across seven sites from Asia, West Africa and East Africa, comprised of 806 *S. flexneri*, 305 *S. sonnei*, 75 *S. boydii* and 60 *S. dysenteriae* (Fig. 1A). To compare the genomic diversity of *Shigella* species, we determined the distributions of pairwise single-nucleotide polymorphism (SNP) distances and scaled the total detected SNPs against the length of the chromosome (in kbp) for each species (Fig. 1B). This revealed that *S. boydii* contained the greatest diversity (24.2 SNPs/kbp), followed by *S. flexneri* (19.5 SNPs/kbp) and *S. dysenteriae* (11.8 SNPs/kbp), with *S. sonnei* being >9.8-fold less diverse (1.2 SNPs/kbp) or >13.1-fold less diverse (0.9 SNPs/kbp) excluding two outliers (see below, Fig. 1B). This revealed that *S. sonnei* caused between 20 and 25-fold more disease relative to genomic diversity than *S. flexneri* and either *S. dysenteriae* or *S. boydii* (Fig. 1B), indicating the value of vaccination against *S. sonnei* as a comparatively conserved target relative to disease burden. Examination of the gene repertoire revealed that this relative chromosomal diversity was consistent with the accessory genome variation among species (fig. S1).

Early global population structure studies revealed that each *Shigella* species is delineated into multiple WGSA subtypes (20-23). Specifically, *S. flexneri* is comprised of seven phylogroups (PGs) (20) and *S. sonnei* of five lineages (24). To describe the genomic epidemiology of the GEMS *Shigella* within existing frameworks we constructed species phylogenetic trees and integrated these with epidemiological metadata and publicly available genomes. The *S. flexneri* phylogeny revealed two distinct lineages separated by ~34,000 SNPs; one comprising five previously described PGs (20) and a distant clade comprised largely of *S. flexneri* serotype 6 isolates (herein termed Sf6), contributing distinctly to the disease burden of each country (Fig. 2 and fig. S2). Phylogenetic analysis of *S. sonnei* revealed that all but two isolates belonged to the globally dominant multidrug resistant (MDR) Lineage III (21) (fig. S3). For *S. boydii* and *S. dysenteriae*, a total of four and two previously described phylogenetic clades (23, 25) were identified, respectively (fig. S4). Marked phylogenetic association of isolates with country of origin prompted an examination of species genomic diversity by region (East Africa, West Africa and Asia) and revealed that while *S. flexneri* diversity was comparable across regions, diversity varied by region for the remaining species (fig. S5). Specifically, *S. sonnei* was more genomically diverse in East Africa owing to the presence of two Lineage II isolates from Mozambique. For *S. boydii*, Asia contained greater diversity than African regions, owing to isolates belonging to additional clades. *S. dysenteriae* diversity was lower in West Africa relative to other regions by virtue of having only one circulating clade. These geographical differences highlight the importance of considering regional variations during vaccine development and that vaccine candidates should be evaluated across multiple regions.

Genomic subgroups as an alternative targeting method

To explore the utility of vaccination targeting genomic subtype (relative to targeting serotype) for *S. flexneri*, we determined the relative effect size of the dominant subtype on the epidemiological outcome of shigellosis (i.e., isolates derived from case patients rather than from controls, as defined in GEMS). The dominant genomic subtype was PG3, which comprised the majority (47%, 378/806) of total isolates, as well as case (50%, 341/687) isolates, with some regional variation (Fig. 2). This resulted in an increased odds of cases (OR = 2.3, 95% CI = 1.5-3.6, *p* = 0.0001) for PG3 compared with other genomic subtypes (PGs and Sf6) (methods, table S3). The association of cases with the dominant serotype, *S. flexneri* serotype 2a (accounting for 29% (234/806) of total isolates and 31% (210/687) of case isolates) also resulted in an increased odds of cases (OR = 1.9, 95% CI = 1.7-3.2, *p* = 0.0099) (table S3). But the higher prevalence and larger effect size of PG3 relative to serotype 2a on case status offers compelling evidence that targeting vaccination by phylogroup might offer broader coverage per licenced vaccine relative to, or in combination with, a serotype-specific approach.

Diversity of S. flexneri relevant to serotype-targeted vaccines

The development of serotype-targeted vaccines is complicated by the diversity and distribution of serotypes, which are heterogenous over time and place (8, 19, 26, 27). Furthermore, genetic determinants of O-antigen modification are often encoded on mobile genetic elements (28, 29) that can move horizontally among bacterial populations, causing the recognised, but poorly quantified phenomenon of serotype switching (20, 27, 28), which may result in the rapid escape of infection induced immunity against homologous serotypes. For our analyses of serotype switching, we focused on *S. flexneri* owing to high disease burden and serotypic diversity. Phenotypic serotyping data were overlaid onto the phylogeny and revealed that while generally there was a strong association of genotype (i.e. PG/Sf6) with serotype (Fisher's exact test; *p*<2.20E-16), multiple serotypes were observed for each genotype (Fig. 3). The greatest serotype diversity was observed in PG3, comprised of seven distinct serotypes and two subserotypes. Correlation of serotypic diversity (number of serotypes) and genomic diversity (maximum pairwise SNP distance within genotype) revealed no evidence for an association, but a significant positive correlation of serotypic diversity with the number of isolates in each genotype was found (fig. S6), indicating that serotype diversity scales with prevalence.

To qualitatively and quantitatively determine serotype switching across *S. flexneri*, we examined the number of switches occurring within each genotype. A switching event was inferred when a serotype emerged (either as a singleton or monophyletic clade) that was distinct from the majority (>65%) serotype within a genotype (Fig. 3 and fig. S7). PG6 was excluded from the analysis, as only three isolates from GEMS belonged to this genotype and a dominant serotype could not be inferred. Quantitatively, this revealed serotype switching was infrequent, with only 26 independent switches (3.3% of isolates) identified across the five *S. flexneri* genotypes. Although the frequency of switching varied across the genotypes, statistical support for an association of serotype switching with genotype fell short of significance (Fisher's exact test; *p* = 0.09). Qualitatively, the majority (22/26) of switching resulted in a change of serotype, with few (4/26) resulting in a change of subserotype**.** Examination of O-antigen modification genes revealed that serotype switching was facilitated by changes in the composition of phage-encoded *gtr* and *oac* genes in the genomes, as well as point mutations in these genes (table S4). Our data also revealed that few (4/26) switching events resulted in more than two descendant isolates (fig. S7). This indicates that while natural immunity drives the fixation of relatively few serotype-switched variants in the short term, the potential pool of variants that could be driven to fixation by vaccine-induced selective pressure following a serotype-targeted vaccination program is much larger.

In order to estimate the likely timeframe over which serotype switching events might be expected to occur, we estimated the divergence time of the phylogenetic branch giving rise to each switching event. To streamline the analysis, we focused on two subclades of PG3, the most prevalent phylogroup, in which seven independent serotype switching events were detected (fig. S8). Based on the timeframes observed within our sample (spanning 4 years from 2007 to 2010), serotype switching was estimated to occur within an average of 348 days, ranging from 159 days (95% highest posterior density [HPD]: 16 - 344) to 10206 days (28 years) (95% HPD: 5494 - 15408) (table S5). Taken together, our data shows that although serotype-switching frequency is low, it can occur over relatively short timeframes and lead to serotype replacement such that non-vaccine serotypes could replace vaccine serotypes following a vaccination program, as has been observed for *Streptococcus pneumoniae* (30, 31). These elucidated serotype switching dynamics (i.e. switching occurring over short timeframes and quantitatively proportional to disease burden) highlights the value of a multivalent vaccine and geographically coordinated implementation of *Shigella* vaccination.

Heterogeneity among Shigella vaccine protein antigens

Conserved antigen-targeted vaccines can overcome some hurdles of serotype-targeted vaccines. Hence, we performed detailed examination of six protein antigens that are currently in development and have demonstrated protection in animal models (Table 1). First, we assessed the distribution of the candidates among GEMS *Shigella* isolates which revealed that the proportional presence of antigens varied across species and with genetic context. Specifically, genes encoded on the virulence plasmid (*ipaB*, *ipaC*, *ipaD*, *icsP*) were present in >85% of genomes for each species with the exception of *S. sonnei* (fig. S9). The low proportion (≤5%) of virulence plasmid encoded genes detected among *S. sonnei* was caused by a similarly low detection of the virulence plasmid among *S. sonnei* (6%), which likely arose due to loss during sub-culture (32). In contrast, the chromosomally encoded *ompA* was present in >98% of all isolates, while the *sigA* gene (carried on the chromosomally integrated SHI-1 pathogenicity island (17)) was present in 99% of *S. sonnei* genomes, but only 63% of *S. flexneri* genomes. Notably, among *S. flexneri* genomes, the *sigA* gene was exclusively found in PG3 and Sf6, and present in >96% of isolates in each genotype) (fig. S2), indicating an appropriate distribution for targeting the two genotypes. Second, we assessed the antigens for amino acid variation and modelled the likely impact of detected variants, as antigen variation may also lead to vaccine escape, as demonstrated for the P1 variant of SARS-CoV2 (33, 34). We determined the distribution of pairwise amino acid (aa) sequence identities per antigen against *S. flexneri* vaccine strains for each species (methods). Overall, sequence identities were >90% but varied with antigen (fig. S9). For example, OmpA was present in the highest proportion of genomes, but showed ~5% sequence divergence, while SigA was present in fewer genomes, but exhibited little divergence (<0.5%) among species. The least conserved sequence was IpaD, ranging from 3 to 7% divergence within species.

Not all antigenic variation will affect antibody binding, so we performed *in silico* analyses of the detected variants to assess whether they may compromise the antigens as vaccine targets. Again, we focused our analyses on *S. flexneri* owing to its high disease burden and the likely complication of serotype-based vaccination strategies for this species. We detected 121 variants across the six antigens, the majority (79%) of which correlated with genotype (i.e. belonging to either PGs 1-5 or Sf6, fig. S11). We then determined if amino acid variants were located in immunogenic regions (i.e. epitope/peptide fragment) (fig. S10) and assessed their potential destabilization of protein structure through *in silico* protein modelling. For IpaB, IpaC and IpaD, the epitopes have been empirically determined (35, 36). The sequence and location of peptide fragments of SigA, IcsP and OmpA used in vaccine development are available (37, 38). Variants located within the immunogenic regions were identified for all antigens relative to PG3 reference sequences (methods, Fig. 4). Only 4 of 121 variants were predicted to be highly destabilising to protein structure, and these occurred in: OmpA (residue 89) at a periplasmic turn, SigA (residues 1233 and 1271) in adjacent extracellular turns in the translocator domain (fig. S12), and in IpaD (residue 247) within a beta-turn-beta motif flanking the intramolecular coiled-coil (Fig. 4). While it remains possible that these mutations could affect antigenicity through the disruption of folding or global stability, it is less likely than if they occurred in immunogenic regions. These results thus indicate that it is less likely that existing natural variation will compromise antigen-based vaccine candidates for *Shigella* compared with serotype-based vaccines. However, our approach is limited and the knowledge base incomplete. For example, there was no suitable template available for IpaC, and some epitopes were predicted to be in membrane regions which should be inaccessible to antibodies, indicating the need for more accurate publicly available protein structures to be developed for many of the vaccine antigen candidates.

Region-specific details of antimicrobials as a stop gap

Until a licensed vaccine is available, we must continue to treat shigellosis with supportive care and antimicrobials, for which the current WHO recommendation is the fluoroquinolone, ciprofloxacin (39). However, FQR *Shigella* is currently on the rise and spreading globally (40). To examine AMR prevalence among GEMS isolates for evaluating treatment recommendations**,** we screened for known genetic determinants (horizontally acquired genes and point mutations) conferring resistance or reduced susceptibility to antimicrobials. Although we used only minimal phenotypic data, phenotypic resistance and genotypic prediction correlate well in *S. flexneri* and *S. sonnei* (41, 42). Our analysis revealed that 95% (1189/1246) of isolates were multidrug resistant (MDR), carrying AMR determinants against three or more antimicrobial classes (Fig 5A). *S. flexneri* exhibited the greatest diversity of AMR determinants, with a total of 45 identified determinants across the population, comprising of 38 AMR genes and 7 point mutations (fig. S13 and table S1), and an extensive AMR genotype diversity of 72 unique resistance profiles (Fig. 5A and fig. S14). In contrast, *S. sonnei* exhibited the least diversity, with only 23 AMR determinants and 21 unique resistance profiles. An intermediate and comparable degree of AMR diversity was observed for both *S. dysenteriae* and *S. boydii*.

Overall, a high frequency of AMR genes conferring resistance against aminoglycoside, tetracycline, trimethoprim, and sulphonamide antimicrobials was observed, while resistance against other antimicrobial classes varied with region and species (Fig. 5B). The extended spectrum beta-lactamase gene *blaCTX-M-15* was detected in a small (9/1246) percentage of isolates, and genes conferring resistance to macrolides and lincosamides were also infrequent (fig. S13), indicating that the recommended second-line treatments likely remain effective antimicrobials (43).

However, higher rates of resistance were found against the first-line treatment. FQR in *Shigella* can be conferred through the acquisition of FQR-genes or, more typically, by point mutations in the chromosomal Quinolone Resistance Determining Region (QRDR) within the DNA gyrase (*gryA*) and the topoisomerase IV (*parC*) genes. Single and double QRDR mutations are known to confer reduced susceptibility to ciprofloxacin and are evolutionary intermediates on the path to resistance, conferred by triple mutations in this region (41, 44). Overall, FQR-genes were uncommon in *S. flexneri* (4%, 33/806), *S. sonnei* (1%, 3/305) and *S. dysenteriae* (7%, 4/60), but were present in 32% (24/75) of *S. boydii*. QRDR mutations were identified in all species (fig. S13), but were more common among *S. sonnei* (65%, 199/305) and *S. flexneri* (54%, 435/806) than compared with *S. boydii* (15%, 11/75) and *S. dysenteriae* (30%, 18/60). Among these, triple QRDR mutations were identified in 13% (106/806) of *S. flexneri* and 14% (44/305) of *S. sonnei*. Analysis of the QRDR mutants across the phylogenies indicate marked convergent evolution toward resistance across the genus. Specifically, all triple QRDR mutant *S. sonnei* belonged to one monophyletic subtype (previously described as globally emerging from Southeast Asia (45)), while three distinct triple QRDR mutational profiles were found across three polyphyletic *S. flexneri* genotypes (Fig. 5C). Thus, the polyphyletic distribution of single, double, and triple QRDR mutants indicates continued convergent evolution of lineages with reduced susceptibility or resistant to FQR.

We then stratified the dataset by geographic region which revealed that FQR were largely associated with isolates from Asia where fluoroquinolones are more frequently used compared to African sites (Fig. 5B) (46), which is consistent with trends observed in atypical enteropathogenic *Escherichia coli* isolated from GEMS (46). Our analyses thus suggest that for the period of GEMS trial (2007 – 2011), 17% (150/881) of *Shigella* isolates from Asia were resistant and 58% (508/881) had reduced susceptibility to the WHO recommended antimicrobial. The high level of reduced susceptibility together with marked convergent evolution toward resistance suggests that management of shigellosis with fluroquinolones at these sites may soon be ineffective and regional antimicrobial treatment guidelines may require updating. These results indicate the value of AMR and microbiological surveillance in LMICs and the control and management of shigellosis will be improved by initiatives such as the Africa Pathogen Genomics Initiative (47) and the WHO Global Antimicrobial Resistance Surveillance System (48).

Conclusions

Pathogen genomics is a powerful tool that has a wide range of applications to help combat infectious diseases. Here, we have applied this tool to an unparalleled systematically collected *Shigella* dataset to characterise the relevant population diversity of this pathogen across LMICs in a pre-vaccine era. Our results revealed that current antimicrobial treatment guidelines for shigellosis should be updated, and that improved surveillance will be essential to guide **antimicrobial stewardship**. This study has also highlighted the urgent need to continue the development of *Shigella* vaccines for children in endemic areas. The genomic diversity in *Shigella* presents a major hurdle in controlling the disease and we have demonstrated the anticipated pitfalls of current vaccination approaches, emphasising the importance of considering the local and global diversity of the pathogens in vaccine design and implementation. Although our results are focused on shigellosis, our approach is translatable to other bacterial pathogens which is particularly relevant as we enter the era of vaccines for AMR.

Materials and Methods

***Dataset*, bacterial isolates and sequencing**

A total of 1,264 *Shigella* isolates from GEMS were under investigation in this study (2, 3). All isolates were derived from stool samples/rectal swabs: their identification, confirmation and isolation have been described previously (19). A total of 1,344 isolates were sequenced at the Earlham institute, with genomic DNA extraction, sequencing library construction and whole genome sequencing carried out according to the Low Input Transposase Enabled (LITE) pipeline described by Perez-Sepulveda *et al* (49). Among these, 225 isolates failed QC with a mean sample depth of coverage <10x and an assembly size of <4MB and were re-sequenced. For these isolates, genomic DNA was re-extracted at the University of Maryland School of Medicine (Baltimore, Maryland) from cultures grown in Lysogeny Broth overnight. DNA was extracted in 96-well format from 100 µL of sample using the MagAttract PowerMicrobiome DNA/RNA Kit (Qiagen, Hilden, Germany) automated on a Hamilton Microlab STAR robotic platform. Bead disruption was conducted on a TissueLyser II (20 Hz for 20 min) instrument in a 96 deep well plate in the presence of 200 µL phenol/chloroform. Genomic DNA was eluted in 90 µl water after magnetic bead clean up and the resulting genomic DNA was quantified by Pico Green. The genomic DNA was shipped to the Centre for Genomic Research (University of Liverpool) for whole genome sequencing. Sequencing library was constructed using NEBNext® Ultra™ II FS DNA Library Prep Kit for Illumina and sequenced on the Illumina® NovaSeq 6000 platform, generating 150bp paired-end reads.

An additional 125 publicly available *Shigella* and *E. coli* reference genomes were included in the analyses. Details of GEMS and reference genomes analysed in this study are listed in table S1 and table S2, respectively.

Sequence mapping and variant calling

Adaptors and low-quality bases were trimmed with Trimmomatic v0.38 (50), reads qualities were assessed using FastQC v0.11.6 (https://www.bioinformatics.babraham.ac.uk/projects/fastqc/) and MultiQC v1.7 (51). Filtered reads were mapped against *Shigella* reference genomes with BWA mem v0.7.17 (52) using default parameters. *S. flexneri*, *S. sonnei*, *S. boydii* and *S. dysenteriae* sequencing reads were mapped against reference genomes from Sf2a strain 301 (accession NC_004337), Ss046 (accession NC_007384), Sb strain CDC 3083-94 (accession NC_010658) and Sd197 (accession NC_007606), respectively. Mappings were filtered and sorted using the SAMtools suite v1.9-47 (53), and optical duplicate reads were marked using Picard v2.21.1-SNAPSHOT MarkDuplicates (http://broadinstitute.github.io/picard/). QualiMap v2.2.2 (54) was used to evaluate mapping qualities and estimate mean sample depth of coverage. Sequencing reads for isolates sequenced using the LITE pipeline and re-sequenced at CGR were combined to increase overall sample depth of coverage. Sequence variants were identified against reference using SAMtools v1.9-47 mpileup and bcftools v1.9-80 (53). Low quality SNPs were filtered if mapping quality <60, Phred-scaled quality score <30 and read depth <4.

Phylogenetic reconstruction and inference of genomic diversity

Filtered SNP variants were used to generate a reference-based pseudogenome for each sample, where regions with depth of coverage >4x were masked in the pseudogenome. Additionally, regions containing phage (identified using PHASTER (55)) and insertion sequences were identified from the reference genomes, and co-ordinates were used to mask these sites on the pseudogenomes using BEDTools v2.28.0 maskfasta (56). For each species, chromosome sequences from the masked pseudogenomes were extracted and concatenated. Gubbins v2.3.4 (57) was used to remove regions of recombination and invariant sites from the concatenated pseudogenomes. This generated a chromosomal SNP alignment length of 78,251 bp for *S. flexneri* (*n*=806), 5,081 bp for *S. sonnei* (*n*=305), 98,842 bp for *S. boydii* (*n*=75) and 45,031 bp for *S. dysenteriae* (*n*=60). Maximum-likelihood phylogenetic reconstruction was performed independently for each species and inferred with IQ-TREE v2.0-rc2 (58) using the FreeRate nucleotide substitution, invariable site and ascertainment bias correction model, with 1000 bootstrap replicates. In order to contextualise GEMS isolates within the established genomic subtypes and to infer the most appropriate root for each species tree, phylogenetic trees were reconstructed including publicly available reference genomes of isolates from previously defined lineages/phylogroups/clades and *E. coli* isolates (table S2). Phylogenetic tree for *S. flexneri*, *S. boydii* and *S. dysenteriae* was rooted using *E. coli* strain

IAI1-117 (accession SRR2169557) as an outgroup, respectively. Phylogenetic tree for *S. sonnei* was midpoint rooted. Visualizations were performed using interactive Tree of Life (iTOL) v6.1.1 (59).

To measure the extent of *shigella* genomic diversity among GEMS population, pairwise SNP distance was determined from the alignment of core genome SNPs identified outside regions of recombination using snp-dists v0.7.0 (https://github.com/tseemann/snp-dists). For each species, the genomic diversity, measured by SNPs per kbp, was determined by dividing the core genome SNP alignment length by the core genome size (*S. flexneri* 4,015,307 bp, *S. sonnei* 4,177,070 bp, *S. boydii* 4,088,693 bp and *S. dysenteriae* 3,821,602 bp). Scaling the proportion of disease burden attributable by the genome diversity of each species, the percentage of species contribution to GEMS shigellosis disease burden was divided by the number of SNPs per kbp.

Serotype switching time frame inference

To estimate the likely time frame of serotype switching, we performed temporal phylogenetic reconstruction in order to infer the time of divergence along branches exhibiting serotype switching. We streamlined the analysis and focused on isolates belonging to two subclades of *S. flexneri* PG3. First, for each of the two subclades (*n*=99 and *n*=45), a maximum-likelihood phylogeny was reconstructed based on genome multiple sequence alignments (described above). Then, TempEst v1.5.3 (60) was used determine if there is sufficient temporal signal in the data by inferring linear relationship between root-to-tip distances of the phylogenetic branches with the year of sample isolation. Data from both subclades revealed positive correlation between sampling time and phylogenetic root-to-tip divergence, with R^2 of 0.186 and 0.111 (fig. S16). Once temporal signals within each of the two datasets were confirmed, core genome SNP alignments of length 559 bp and 1,244 bp were analysed independently using BEAST2 v2.6.1 (61). The parameters were as follows: dates specified as days, bModelTest (62) implemented in BEAST2 was used to infer the most appropriate substitution model, a relaxed log normal clock rate with a coalescent Bayesian skyline model for population growth. A total of five independent chains were performed, each with chain length of 250,000,000, logging every 1,000 and accounting for invariant sites. Convergence of each run was visually assessed with Tracer v1.7.1 (63), with all parameter effective sampling sizes ≥200. Tree files were sampled and combined using LogCombiner v2.6.1, the combined files were then summarised using TreeAnnotator v2.6.0 with 10% burn-in to generate Maximum Clade Credibility tree (64). Divergence time was inferred by reading the branch length from the most recent common ancestor to the first sampled isolate that serotype-switched.

Genome assembly and annotation

Draft genome sequences were assembled using Unicycler v0.4.7 (65) with –min_fasta_length set to 200. QUAST v5.0.2 (66) was used to assess the qualities of the assemblies. Assemblies with total assembly length outside the range of <4Mbp and >6.4Mbp were removed. Resulting in an average length of 4,275,508 bp (range: 4 4,004,109 – 4,538,734 bp) for *S. flexneri*, 4,264,097 bp (range: 4,008,630 – 4,779,279 bp) for *S. sonnei*, 4,227,671 bp (range: 4,000,714 – 4,689,815 bp) for *S. boydii* and 4,297,921 bp (range: 4,040,642 – 4,659,860 bp) for *S. dysenteriae*. An average N50 value of 29,804 bp (range: 6,810 – 34,658 bp) was generated for *S. flexneri*, 23,961 bp (range: 11,547 – 30,008 bp) for *S. sonnei*, 20,835 bp (range: 15,323 – 40,119 bp) for *S. boydii* and 22,137 bp (range: 14,090 – 31,358 bp) for *S. dysenteriae*. Draft genomes were annotated using Prokka v1.13.3 (67).

Pangenome analysis

The pangenome of each species was defined using Roary v3.12.0 (68) without splitting paralogues. The pangenome accumulation curves were generated separately for each species using the specaccum function from Vegan v2.5-7 (https://github.com/vegandevs/vegan/), with 100 permutations and random subsampling. Inspections of the variable gene content showed that all four species had open pangenomes, implying that the number of unique gene count increases with the addition of newly sequenced genomes.

Shigella flexneri molecular serotyping

Shigella serotype data was provided by collaborators at the University of Maryland School of Medicine (Baltimore, Maryland), serotyping was performed as previously describe (19). *In silico* serotyping of *S. flexneri* genomes was performed using ShigaTyper v1.0.6 (69) which detects the presence of serotype-determining genetic elements from sequencing reads to predict serotype. ShigaTyper predictions were 84%

concordant to the serotype data provided. SRST2 v2 (70) was used to detect mutations within serotype-determining genetic elements, run against ShigaTyper sequence database with default parameters.

Protein antigen screening

To determine the presence of antigen vaccine candidates among GEMS *Shigella* isolates, genes of the antigen vaccine candidates was screened against draft genome assemblies using screen_assembly (17) with a threshold of ≥80% identity and ≥70% coverage to the reference sequence. Reference sequences for *ipaB*, *ipaC*, *ipaD* and *icsP* were derived from *S. flexneri* 5a strain M90T (accession GCA_004799585) and *ompA* and *sigA* was derived from *S. flexneri* 2a strain 2457T (accession NC_004741), both strains are commonly used in the laboratory for vaccine development. Antigen sequence variations were determined by examining the BLASTp (71) percentage identity against relevant query reference sequence. Allelic variations of antigen vaccine candidates among *S. flexneri* population were identified manually by visualising amino acid sequence alignments using AliView v1.26 (72).

Protein antigen modelling

In order to assess the effect of point mutations on protein stability and vaccine escape, six antigen candidates from *S. flexneri* PG3 were modelled: OmpA, SigA, IcsP, IpaB, IpaC and IpaD (Table 1). PG3 was selected as it is the most prevalent phylogroup and is therefore the target of current vaccine development. To model the antigen targets, we first searched for a suitable template using HHPred (73, 74). Five of the six proteins (OmpA, SigA, IcsP, IpaB and IpaD) had suitable homologues available. To improve the performance of the comparative modelling, the signal peptides for OmpA, SigA and IcsP were removed and OmpA, SigA and IpaB were modelled in two parts to make use of optimal templates. RosettaCM (75) was used to generate 200 models for each of the five proteins using the single best available template. For IpaC, where no suitable templates were available, trRosetta (76) was used to create five de novo predicted models. The best model for each antigen candidate was selected using QMEAN's average local score. QMEANbrane (77, 78) was used for suitable membrane proteins (IpaB, IpaC & IpaD), otherwise QMEANDisCo (77) was used (table 6). Full details of the modelling and ranking are shown in table 7. The effect of point mutations on the stability of the antigen candidates was assessed using PremPS, and the default criterion of ($\Delta\Delta G > 1$ kcal mol^{-1}) used to defining highly destabilising mutations (79).

Detection of AMR genetic determinants and AMR testing

To detect the presence of known genetic determinants for AMR, AMRFinderPlus v3.9.3 (80) was used to screen draft genome assemblies against the AMRFinderPlus database, which is derived from the Pathogen Detection Reference Gene Catalog (https://www.ncbi.nlm.nih.gov/pathogens/). AMRFinderPlus was performed with the organism-specific option for *Escherichia*, to screen for both point mutations and genes, and filter out uninformative genes that were nearly universal in a group. Output was then filtered to remove genetic determinants identified with ≤80% coverage and ≤90% identity. The presence of *S. sonnei* virulence plasmid was confirmed using short-read mapping using BWA mem (as described above) against the reference virulence plasmid from Ss046 (GenBank accession CP000039.1). Presence of the plasmid was defined by mapping of >60% breadth of coverage across the reference. Visualisations of AMR resistance profiles were performed with UpSetR v2.1.3 (81). Four *S. flexneri* isolates with triple QRDR mutations were phenotypically tested for ciprofloxacin resistance using the Kirby-Bauer standardized disk diffusion method (82).

Statistical analyses

The strength of association between *S. flexneri* genomic subtype and serotype with the occurrence of case outcome was calculated using MedCalc's odds ratio calculator v20 (https://www.medcalc.org/calc/odds_ratio.php) to report the odds ratio, 95% confidence interval and statistical association. Association of genomic subtype with serotype and serotype switching was tested using Fisher's exact test. Linear regression analysis was used to determine the correlation between serotype diversity to various properties of genomic subtype. Both analyses were performed using R v4.0.3.

Acknowledgements

We acknowledge and thank members of Baker group and Lab H at the University of Liverpool, and Rodrigo Bacigalupe at KU Leuven for invaluable discussions. We also thank Jay Hinton and Blanca Perez Sepulveda for logistical support orchestrating the thermolysate shipping. The authors are grateful to Sam Haldenby, Matthew Gemmell and Richard Gregory and the Centre for Genomics Research, University of Liverpool for technical support. The authors acknowledge Dr. Irene Kasumba, Ms. Jennifer Jones, Mr. Sunil Sen and Ms. Jasnehta-Permala-Booth for preparing GEMS *Shigella* isolates for sequencing and antimicrobial testing. **Funding**: This work was supported by a UKRI MRC NIRG award (MR/R020787/1), a technology directorate voucher from the University of Liverpool, by the National Institute of Allergy and Infectious Diseases, National Institutes of Health, Department of Health and Human Services under grant number U19AI110820, and by both a Global Challenges Research Fund (GCRF) data and resources grant BBS/OS/GC/000009D and the BBSRC Core Capability Grant to the Earlham Institute BB/CCG1720/1. Next-generation sequencing and library construction were delivered via the BBSRC National Capability in Genomics and Single Cell (BB/CCG1720/1) at Earlham Institute, by members of the Genomics Pipelines Group. RJB is funded by a Biotechnology and Biological Sciences Research Council Doctoral Training Partnership studentship (BB/M011186/1). KSB is supported by a Wellcome Trust Clinical Research Career Development Award (106690/A/14/Z) and an Academy of Medical Sciences Springboard award (SBF002/1114), and is affiliated to the National Institute for Health Research Health Protection Research Unit (NIHR HPRU) in Gastrointestinal Infections at University of Liverpool in partnership with Public Health England (PHE) and collaboration with University of Warwick. The views expressed are those of the author(s) and not necessarily those of the NHS, the NIHR, the Department of Health and Social Care or Public Health England. **Competing interests**: The authors declare no competing interests. **Data and materials availability**:

Author contributions

R.J.B performed majority of the data analysis and interpretation of the results under the scientific guidance of K.S.B. A.J.S and D.J.R performed *in silico* protein antigens modelling and prediction of the impacts of amino acid substitutions on protein stability. C.V.P supported Bayesian Evolutionary Analysis by Sampling Trees. S.M.T. prepared and provided GEMS *Shigella* isolates and metadata. DR contributed to sample preparation. R.J.B and K.S.B drafted the manuscript. All authors contributed to editing of the manuscript.

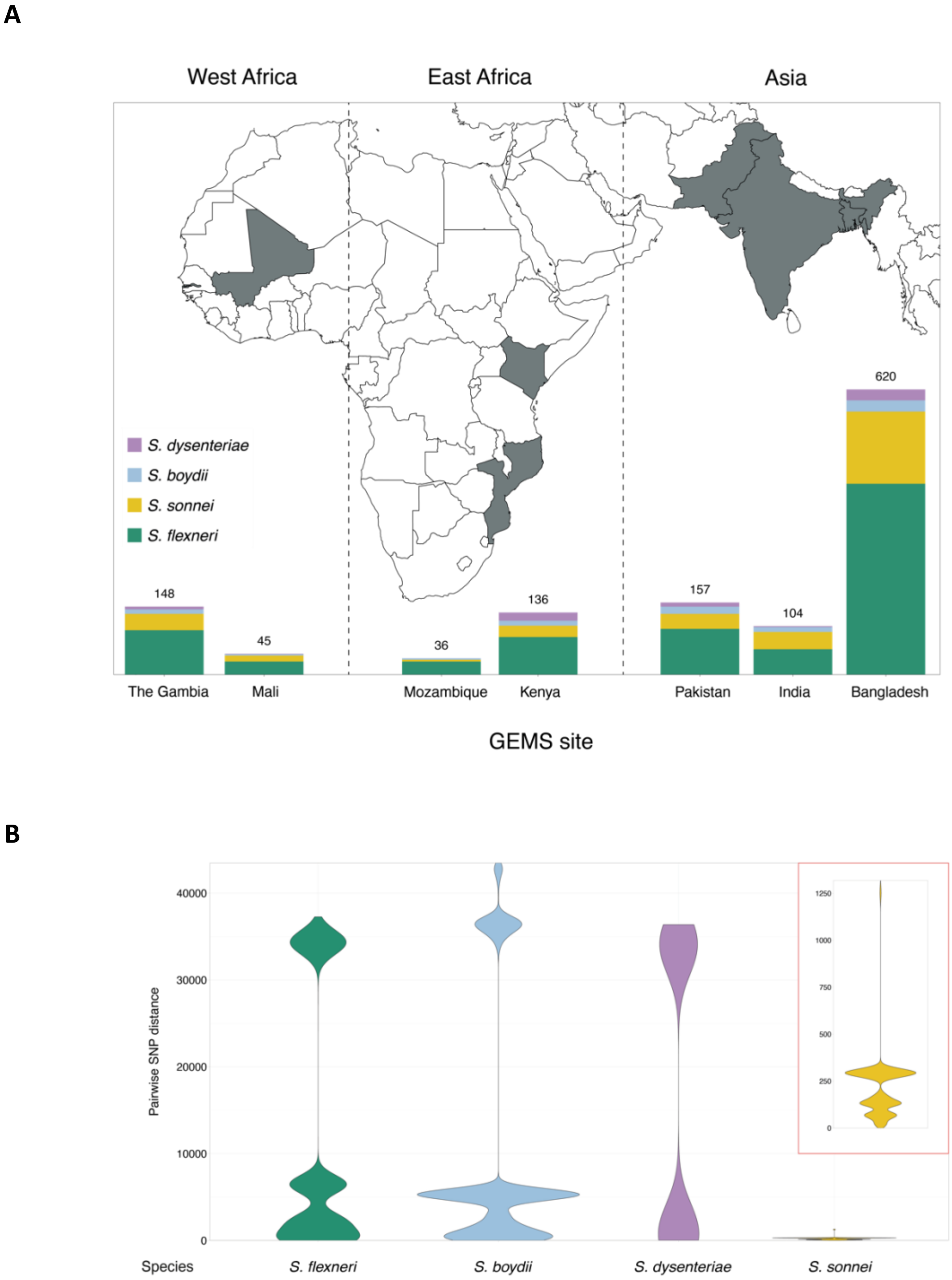

Species	*S. flexneri*	*S. boydii*	*S. dysenteriae*	*S. sonnei*
Genomic diversity (SNPs / kbp)	19.5	24.2	11.8	1.2 (0.9)
Attributable shigellosis (%)	65.9	5.4	0.5	23.9
Attributable shigellosis / Genomic diversity	3.4	0.2	0.04	19.9 (26.6)

Fig. 1. The diversity of *Shigella* spp. across seven LMIC. (**A**) Stacked bar graphs illustrate the number of isolates from each *Shigella spp.* sequenced from GEMS and used in the current study, grouped by study sites. (**B**) Pairwise genomic distances (in SNPs) among *Shigella* isolates within subgroups are shown as violin plots. A magnified plot for *S. sonnei* is displayed inside the red box. The table below the plots demonstrates for each species the genomic diversity (as measure by total number of SNPs per kbp [methods]), the contribution to GEMS shigellosis burden and the shigellosis burden relative to genomic diversity. For *S. sonnei*, the genomic diversity and shigellosis burden relative to genomic diversity that was calculated excluding the two outliers are shown in bracket.

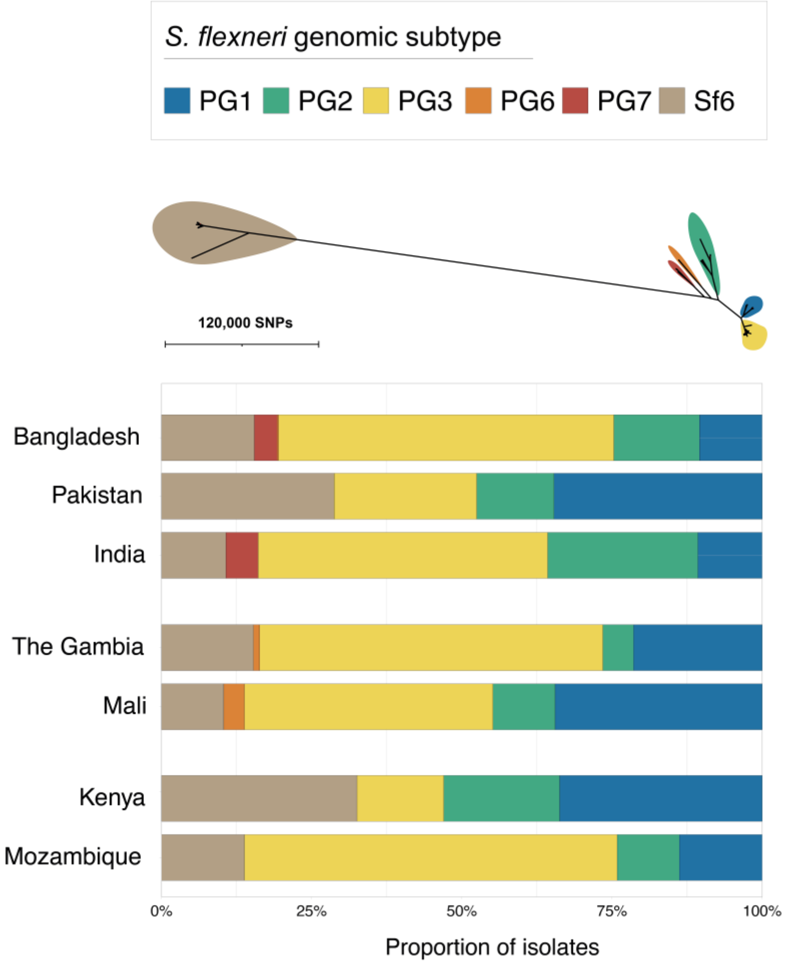

Fig. 2. The diversity of *S. flexneri* genomic subtypes across seven GEMS study sites. An unrooted ML phylogenetic tree of *S. flexneri* genomes identified six distinct genomic subtypes, each highlighted in a different colour according to the inlaid key displayed above the tree. The bar plot below the tree demonstrates the relative frequencies of the subtypes at each study site.

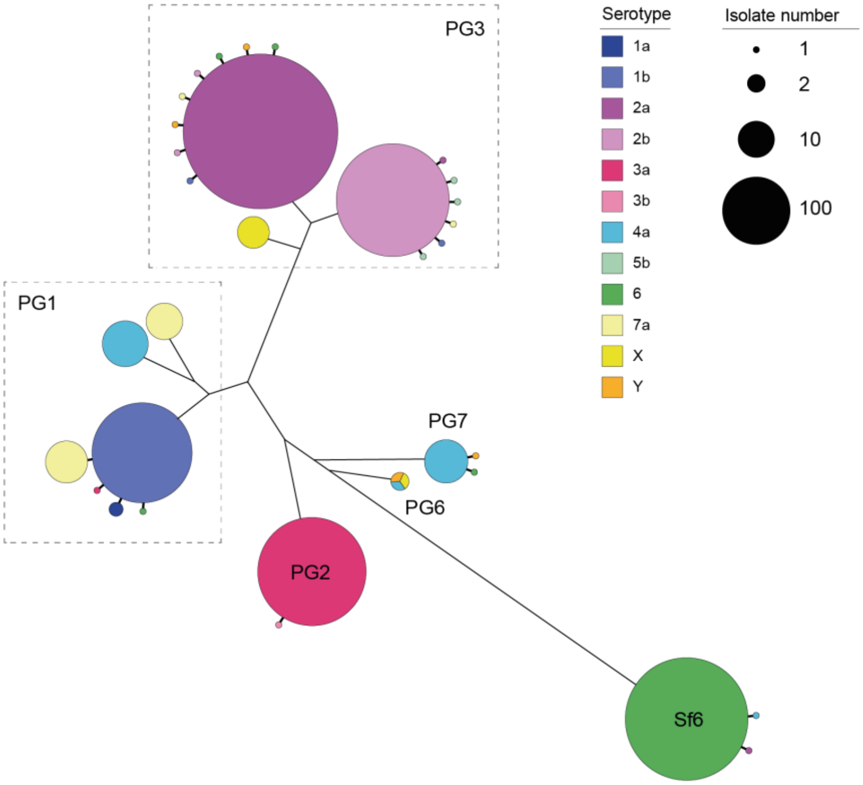

502 **Fig. 3. Diversity of *S. flexneri* population with respect to serotype switching.** The unrooted *S. flexneri* phylogenetic tree is shown with the five phylogroups (PG1-PG7) and Sf6 labeled accordingly. For each genomic subtype, monophyletic clusters of the dominant serotype are shown collapsed into bubbles coloured according to the inlaid key. Single isolates or groups of isolates within a subtype of an alternative serotype are represented by further branches, indicating a single serotype switch. The number of isolates within a single cluster is represented through bubble size.

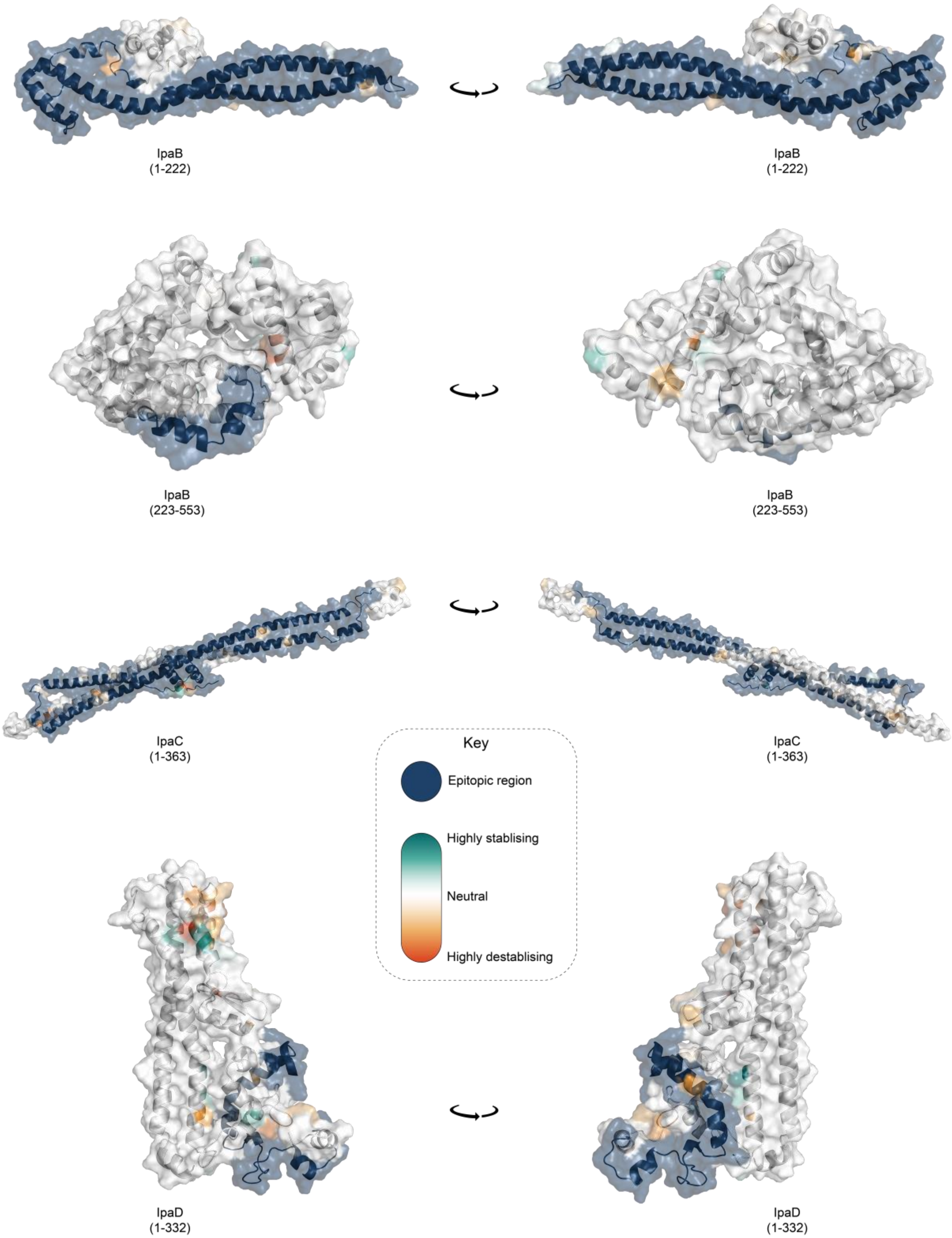
IpaB
(1-222)
IpaB
(1-222)
IpaB
(223-553)
IpaB
(223-553)
IpaC
(1-363)
IpaC
(1-363)
Key
Epitopic region
Highly stablising
Neutral
Highly destablising
IpaD
(1-332)
IpaD
(1-332)

Fig. 4. Visualization of mutations and its predicted effect on modeled IpaB, IpaC and IpaD protein antigens. Visualisation of mutations on modelled proteins IpaB, IpaC and IpaD. The protein residue ranges modelled are shown in brackets. Blue region represents empirically determined epitopes. Mutations identified within the proteins are coloured using the scale shown in the inlaid key, where highly destabilising mutations are dark orange and highly stabilising mutations are dark green.

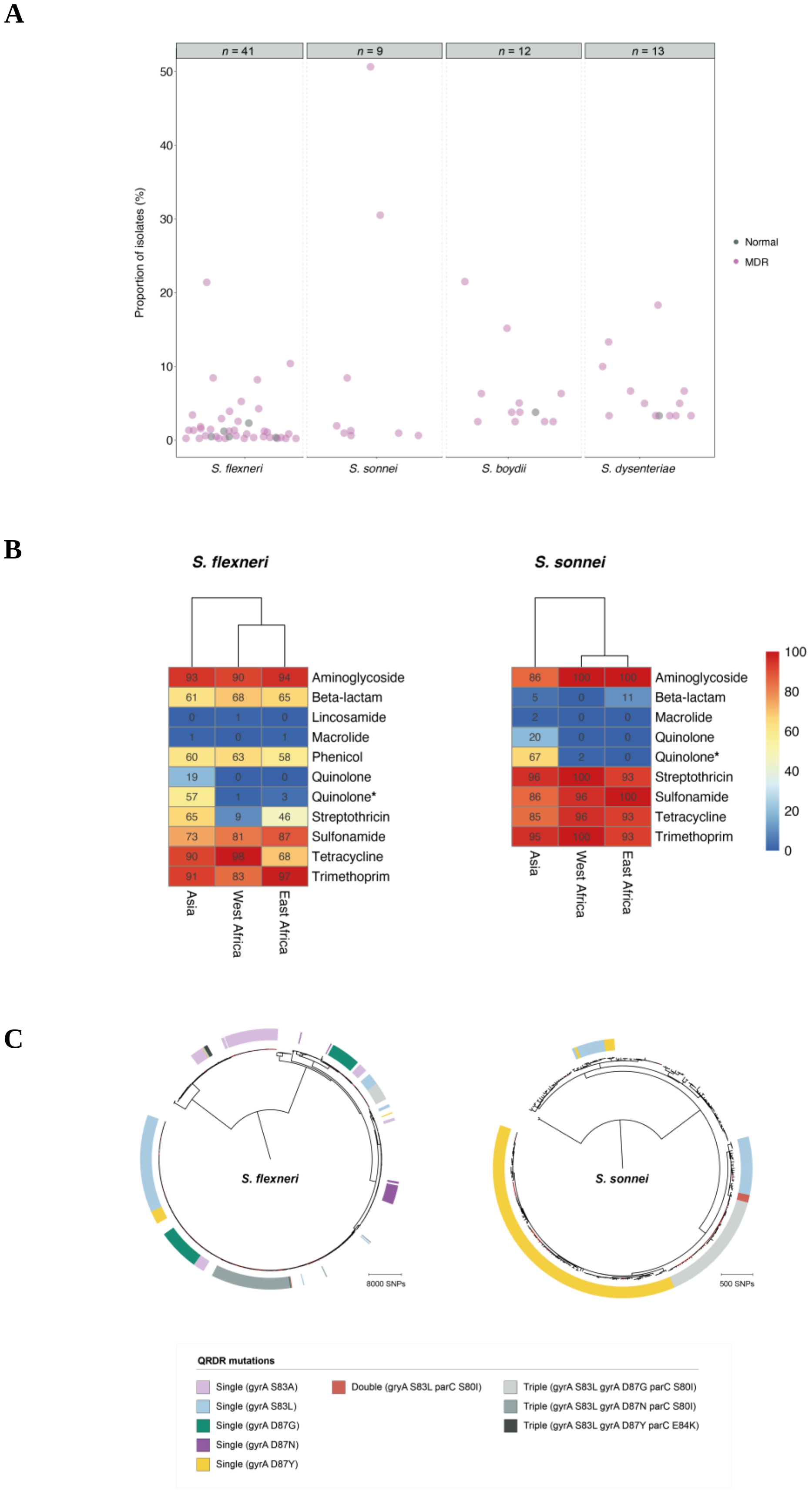
A
n = 41
n = 9
n = 12
n = 13
Proportion of isolates (%)
0
10
20
30
40
50
S. flexneri
S. sonnei
S. boydii
S. dysenteriae
Normal
MDR
B
S. flexneri
93 90 94 Aminoglycoside
61 68 65 Beta-lactam
0 1 0 Lincosamide
1 0 1 Macrolide
60 63 58 Phenicol
19 0 0 Quinolone
57 1 3 Quinolone*
65 9 46 Streptothricin
73 81 87 Sulfonamide
90 98 68 Tetracycline
91 83 97 Trimethoprim
Asia
West Africa
East Africa
S. sonnei
86 100 100 Aminoglycoside
5 0 11 Beta-lactam
2 0 0 Macrolide
20 0 0 Quinolone
67 2 0 Quinolone*
96 100 93 Streptothricin
86 96 100 Sulfonamide
85 96 93 Tetracycline
95 100 93 Trimethoprim
Asia
West Africa
East Africa
100
80
60
40
20
0
C
S. flexneri
8000 SNPs
S. sonnei
500 SNPs
QRDR mutations
Single (gyrA S83A)
Single (gyrA S83L)
Single (gyrA D87G)
Single (gyrA D87N)
Single (gyrA D87Y)
Double (gryA S83L parC S80I)
Triple (gyrA S83L gyrA D87G parC S80I)
Triple (gyrA S83L gyrA D87N parC S80I)
Triple (gyrA S83L gyrA D87Y parC E84K)

Fig. 5. AMR genotypic profile diversity and convergent evolution of ciprofloxacin resistance. (**A**) Frequencies of AMR genotypic profiles among *Shigella* spp. Each point in the scatterplot represents a unique AMR genotype profile: the proportion of isolates with a particular profile is displayed along the y-axis. Profiles identified in only a single isolate are not displayed. MDR genotypic profile conferring resistance or reduced suppressibility to three or more drug classes are highlighted in pink, and normal AMR genotype profile conferring resistance or reduced suppressibility in fewer than three drug classes are in grey. Numbers displayed above the plot represents the number of AMR genotype profiles plotted for each species. (**B**) Detection of known AMR genetic determinants associated with drug class grouped by country. Each cell in the heatmap represents the percentage of isolates from a region containing genetic determinants associated with resistance to a drug class. Genetic determinant conferring reduced susceptibility to quinolone is indicated with an asterisk. (**C**) The genetic convergent evolution of ciprofloxacin resistance in *S. flexneri* and *S. sonnei*. The presence of multiple monophyletic clades of QRDR mutations (single, double, or triple according to the inlaid key) conferring reduced susceptibility or resistance to ciprofloxacin is shown in the outer ring. B and C for *S. boydii* and *S. dysenteriae* are shown elsewhere (fig. S15).

Table 1. *Shigella* antigen vaccine candidates examined in the current study.

Vaccine candidate	**Development stage**	**Location**	**Reference**
IcsP (OmpP)	Preclinical	Virulence plasmid	Czerkinsky and Kim (*37*)
SigA	Preclinical	Chromosome (pathogenicity island)	Czerkinsky and Kim (*37*)
IpaB	Phase I	Virulence plasmid	Martinez-Beccera (*16*); Riddle et al (*83*); Tribble et al (*84*)
IpaC			
IpaD			
OmpA	Preclinical	Chromosome	Pore *et al* (*85*)

A

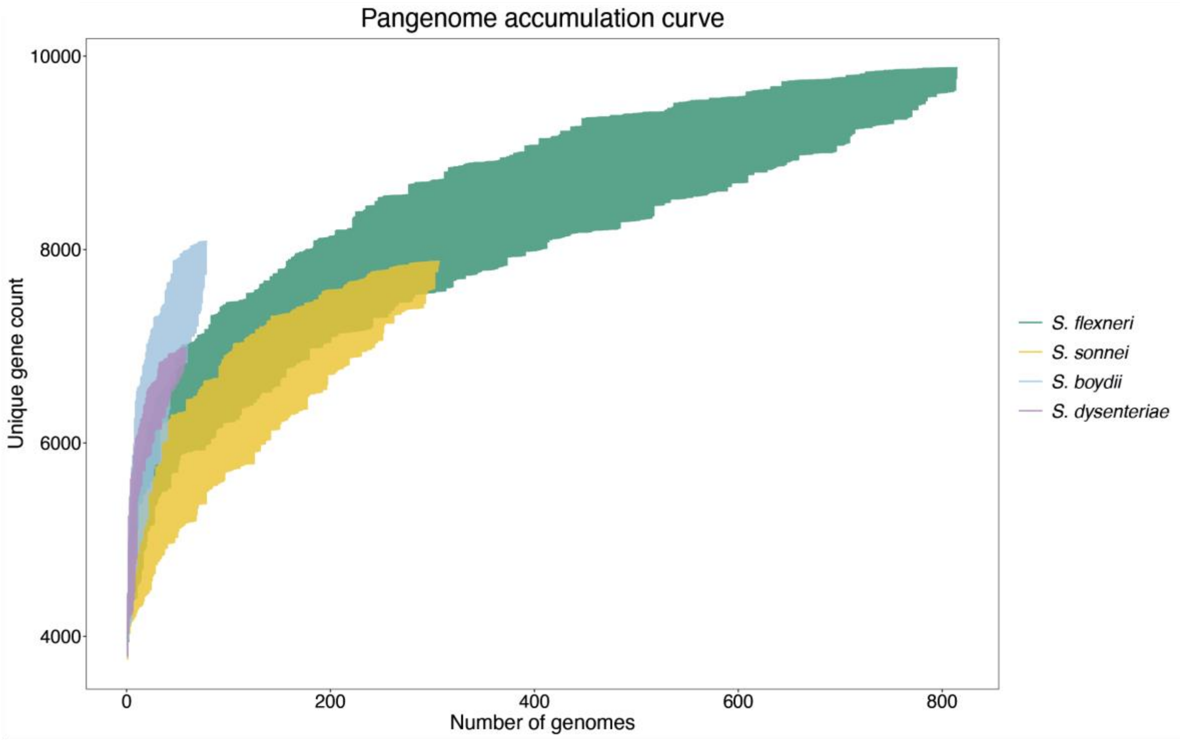
Pangenome accumulation curve
Unique gene count
10000
8000
6000
4000
0
200
400
600
800
Number of genomes
S. flexneri
S. sonnei
S. boydii
S. dysenteriae

B

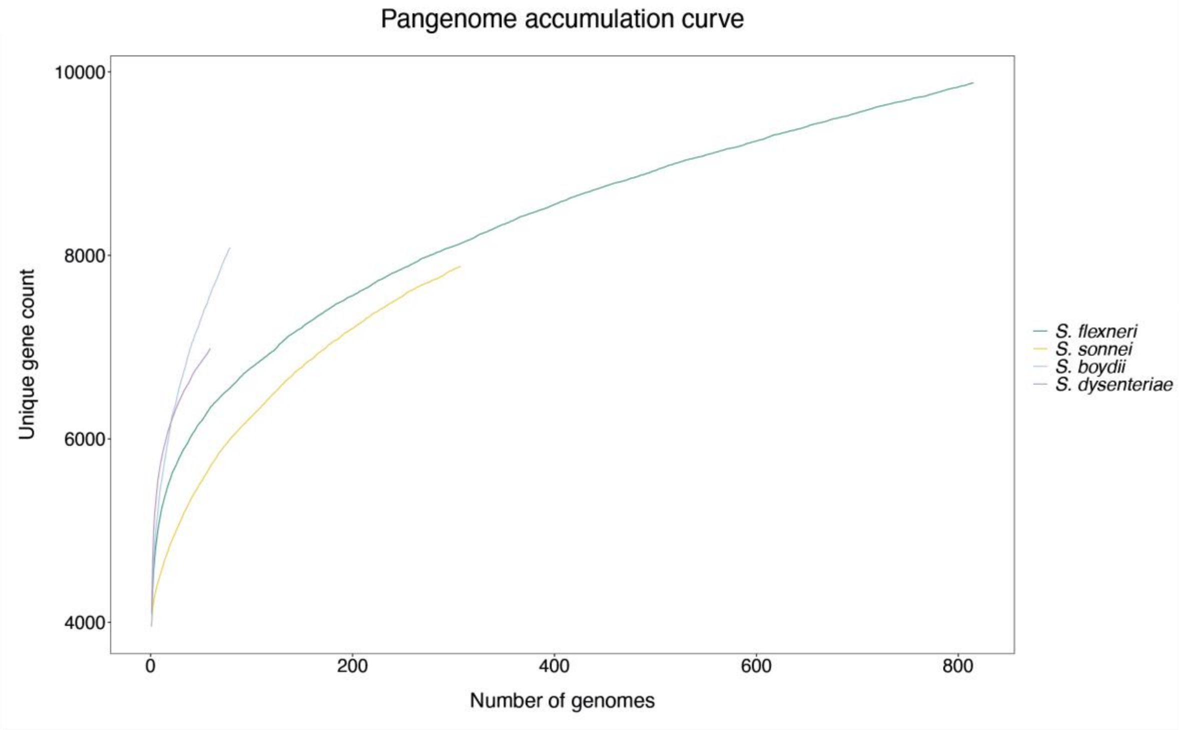
Pangenome accumulation curve
Unique gene count
10000
8000
6000
4000
0
200
400
600
800
Number of genomes
S. flexneri
S. sonnei
S. boydii
S. dysenteriae

531

Fig. S1.

Pangenome accumulation curve of *S. flexneri*, *S. sonnei*, *S. boydii* and *S. boydi*. Each curve demonstrates the number of unique protein coding genes in the pangenome as a new genome is randomly added, with the number of genomes plotted along the x-axis. Random permutation of the data were subsampled 100 times, in which genomes are subsampled without replacement at each iteration. The y-axis shows the minimum and maximum range of unique gene count after each iteration in (A) and the mean value in (B).

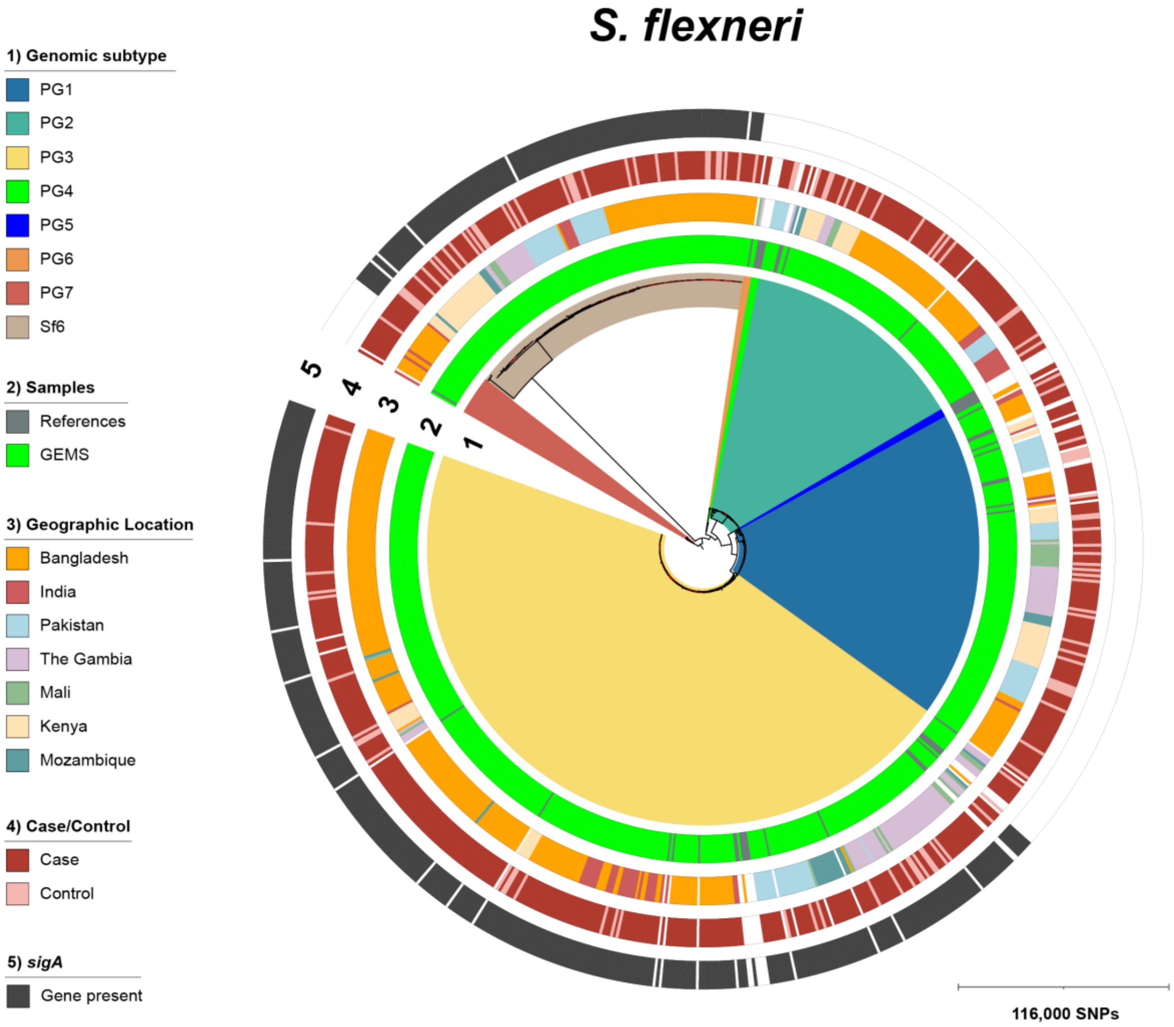

Fig. S2.

Phylogeny of *S. flexneri* population from GEMS. ML phylogenetic tree constructed using core genome SNPs from alignments of 817 *S. flexneri* genomes from GEMS and publicly available genomes. Tree was rooted using *E. coli* genome. The outer concentric rings illustrate different genotypic and epidemiological data according to the numbered inlaid keys displayed next to the tree. Scale bars represents the number of SNPs.

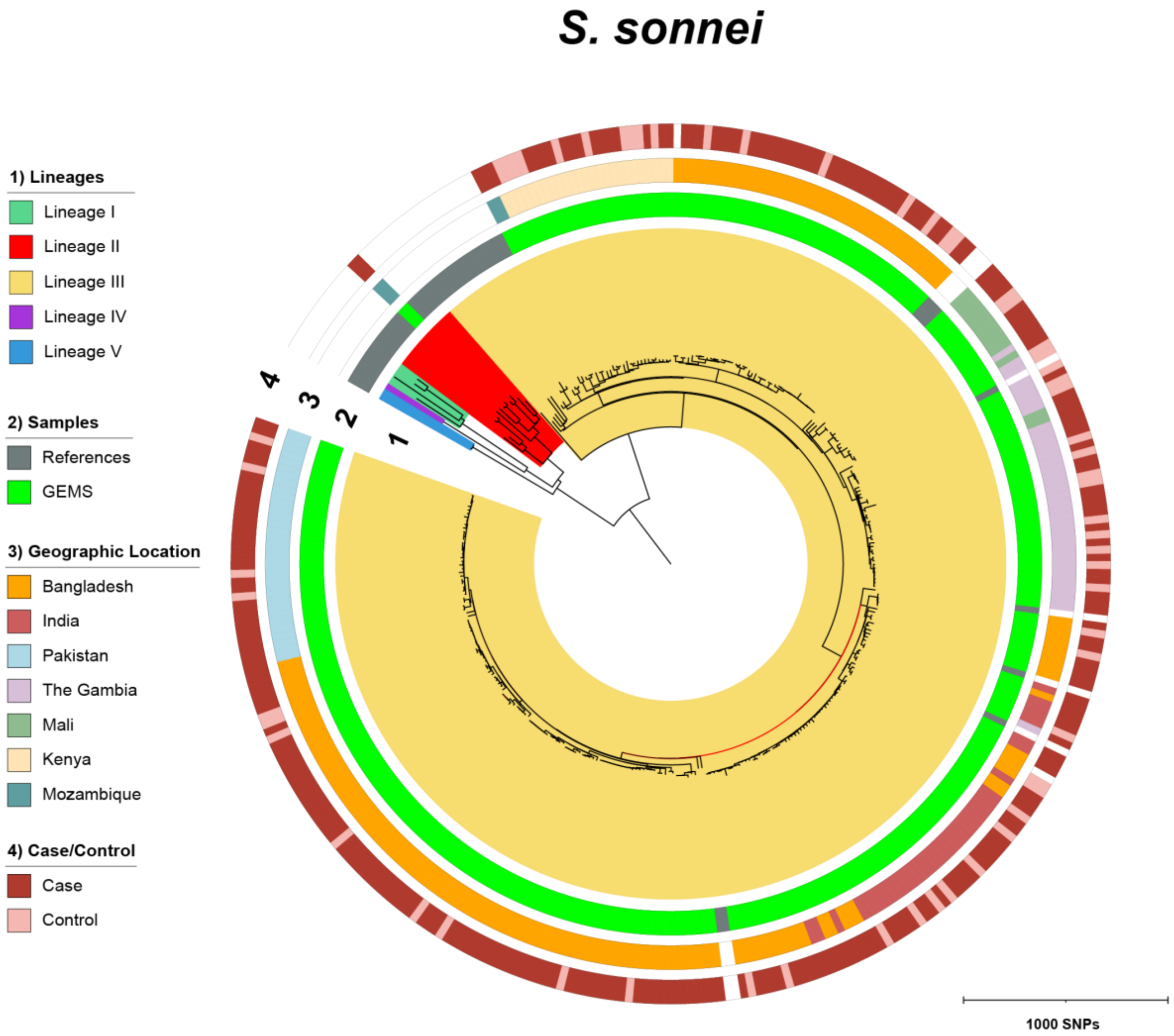

545

546 **Fig. S3.**

547 **Phylogeny of *S. sonnei* population from GEMS.** Midpoint rooted ML phylogenetic tree constructed using core genome SNPs from alignments of 308 *S. sonnei* genomes from GEMS and publicly available genomes.

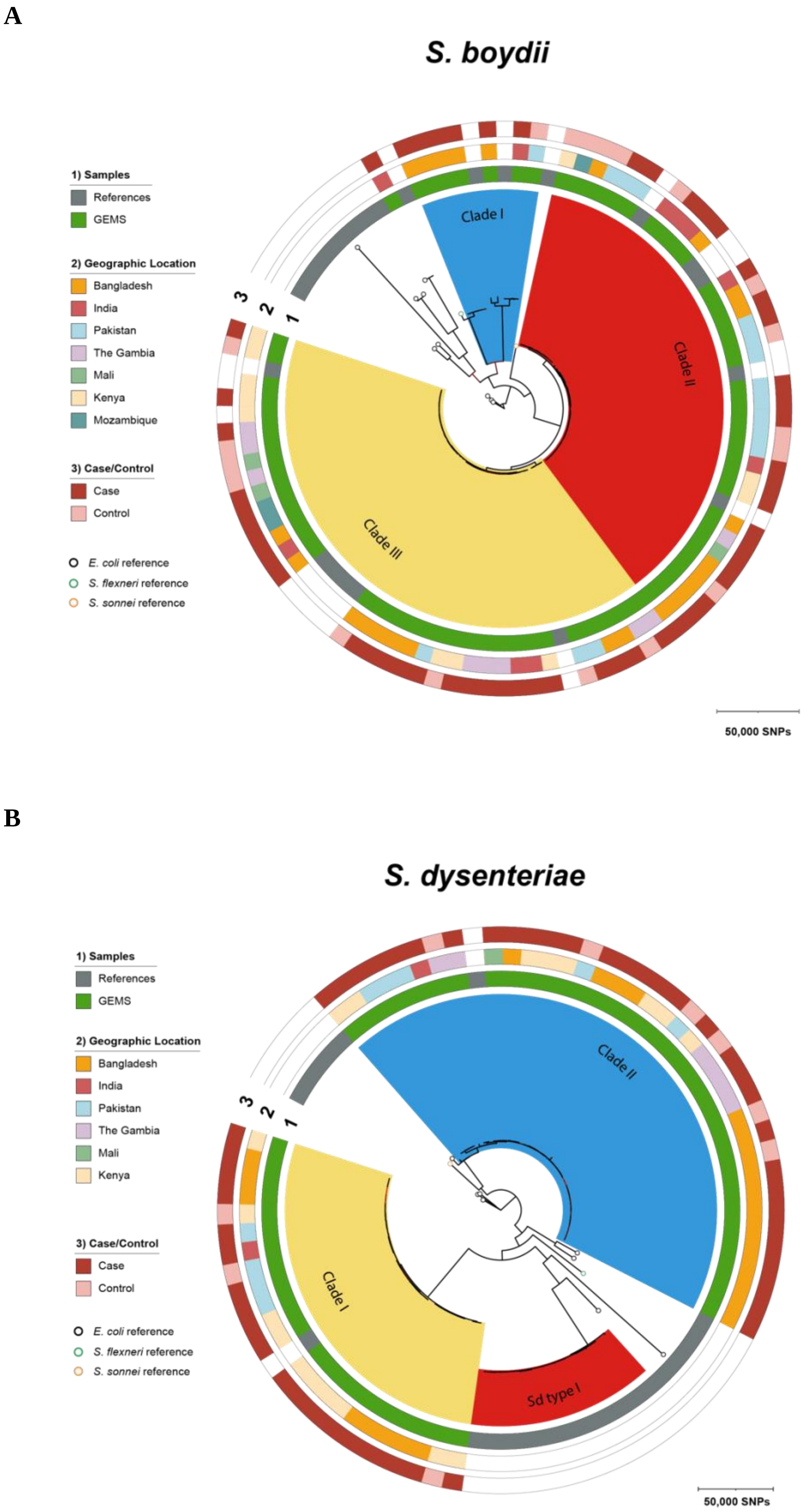
A
S. boydii
1) Samples
References
GEMS
2) Geographic Location
Bangladesh
India
Pakistan
The Gambia
Mali
Kenya
Mozambique
3) Case/Control
Case
Control
E. coli reference
S. flexneri reference
S. sonnei reference
3
2
1
Clade I
Clade II
Clade III
50,000 SNPs
B
S. dysenteriae
1) Samples
References
GEMS
2) Geographic Location
Bangladesh
India
Pakistan
The Gambia
Mali
Kenya
3) Case/Control
Case
Control
E. coli reference
S. flexneri reference
S. sonnei reference
3
2
1
Clade II
Clade I
Sd type I
50,000 SNPs

Fig. S4.

Phylogeny of *S. boydii* and *S. dysenteriae* population from GEMS. ML phylogenetic trees were constructed based on core genome SNPs outside region of recombination from alignments of (A) 79 *S. boydii* and (B) 60 *S. dysenteriae* genomes from GEMS and publicly available genomes. Both trees were rooted using *E. coli* genome. Scale bar represent number of SNPs.

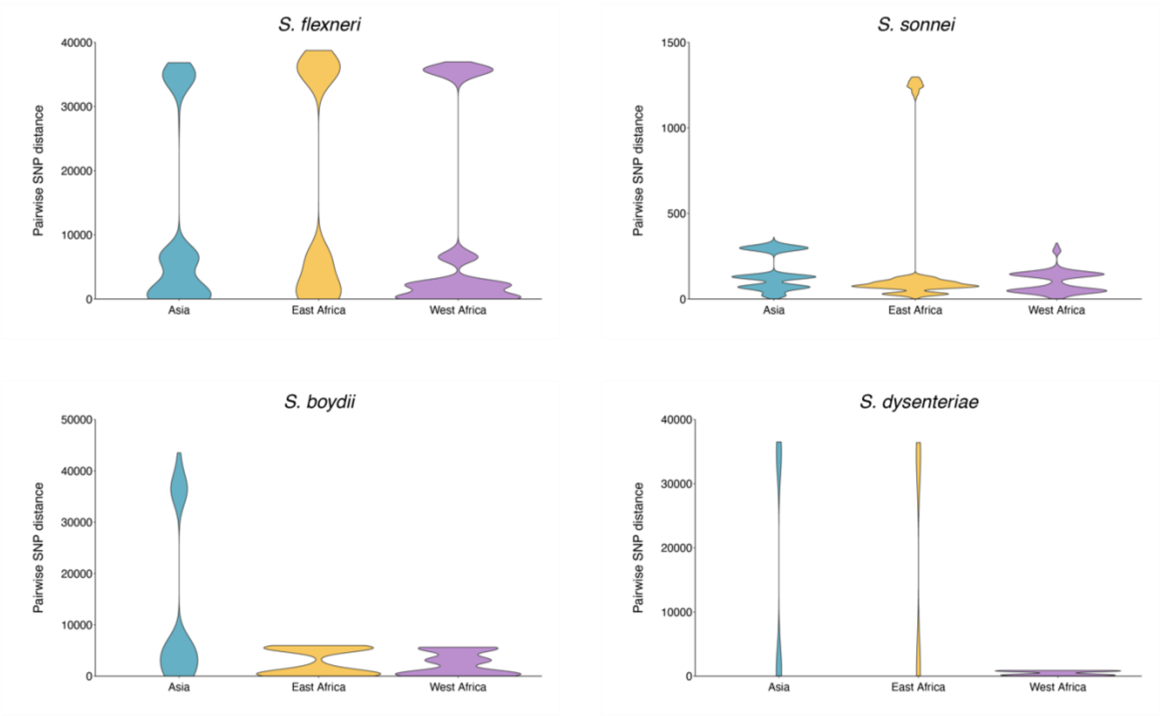

Fig. S5.

Regional diversity of Shigella spp. Comparison of genomic diversity, as measured by pairwise core SNP distance, across GEMS study sites (Asia: Bangladesh, India and Pakistan; East Africa: Kenya and Mozambique; West Africa: The Gambia and Mali) for *S. flexneri*, *S. sonnei*, *S. boydii* and *S. dysenteriae*.

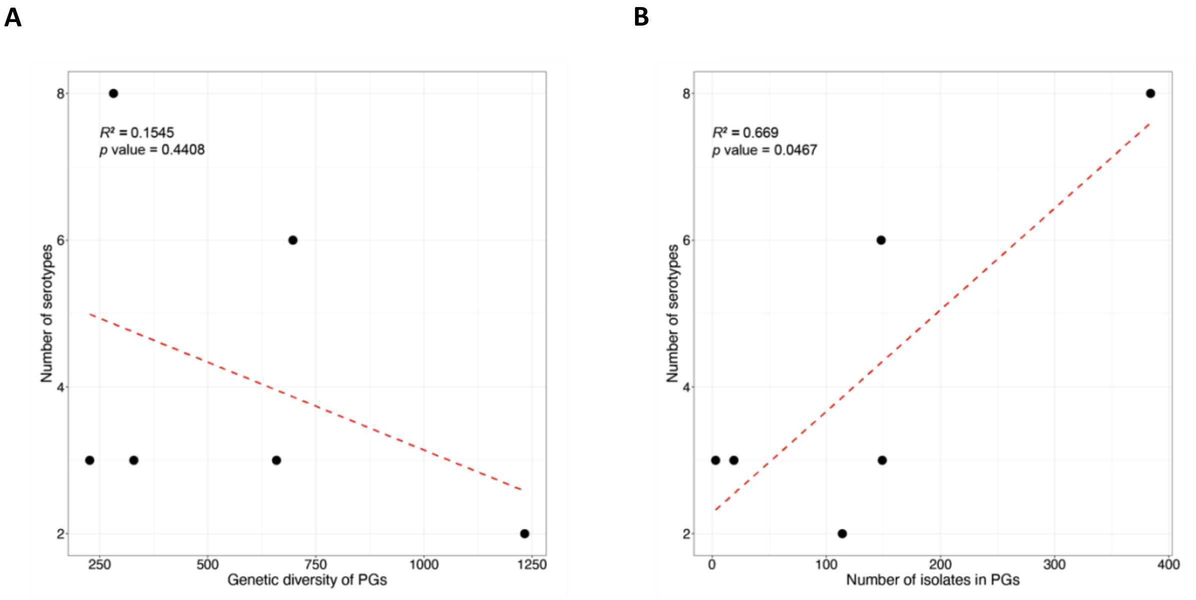

Fig. S6.

Association of *S. flexneri* serotype diversity with different properties of a genomic subtype. For each of the six subtypes identified among *S. flexneri* (PG1-PG7 and Sf6), the number of different serotypes is displayed along the y-axis and plotted against (A) the number of isolates within the subtype and (B) the genetic diversity of the subtype, as measured by pairwise core SNP distance and plotted along the x-axis. Linear regression analysis was performed to assess the association between serotype diversity and the different properties of subtypes. The regression coefficient of determination (R^2) and *p*-value are displayed on the top left of each plot.

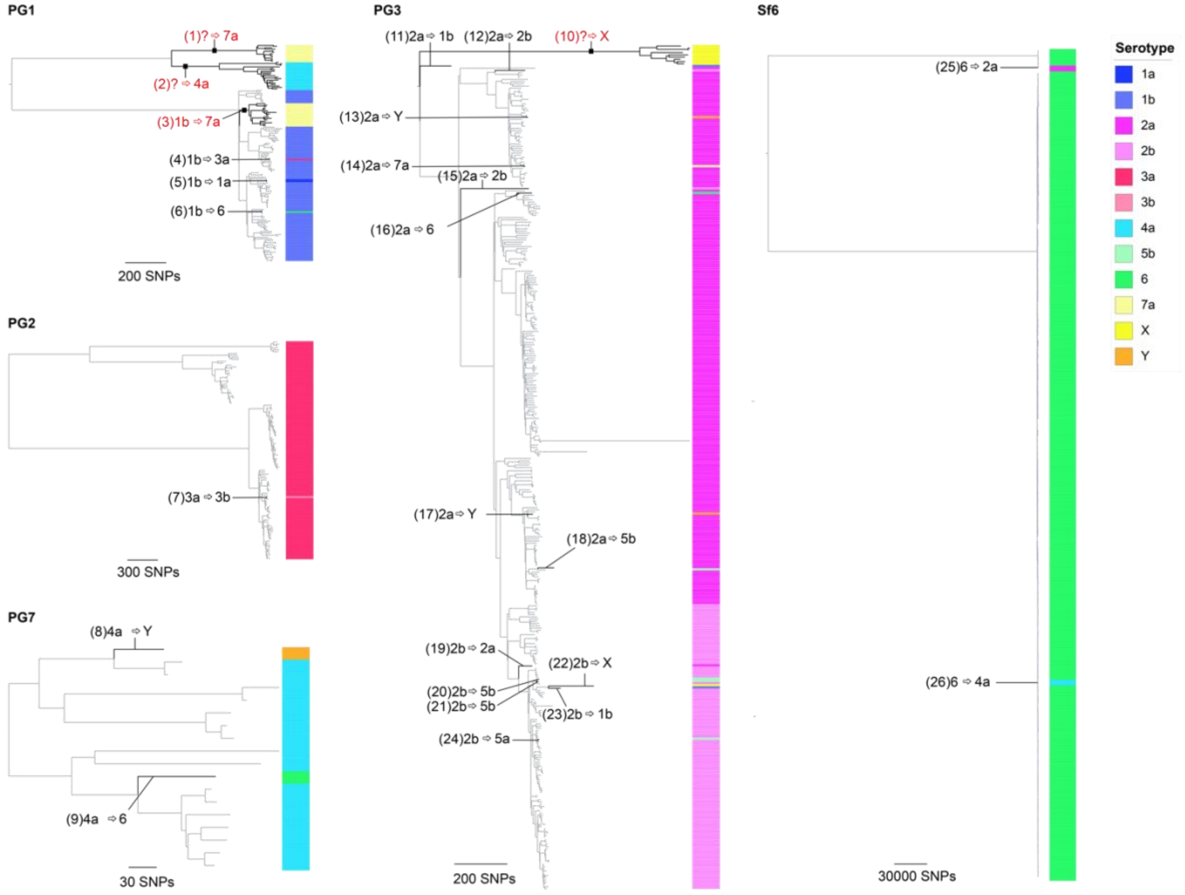

Fig. S7.

Serotype switching events across *S. flexneri* genomic subtypes. ML phylogenetic tree of each subtype was generated based on core genome SNPs. Serotypes determined through biochemical serotyping are displayed on the right-hand side of each tree, and coloured according to the inlaid key. The 26 inferred serotype switching events occurring along the phylogenetic branches are labelled accordingly. Numbers inside each backets represents switch IDs, with further details provided in table S3. Where the dominant serotype cannot be determined, a question mark is displayed, indicating switch from unknown ancestral type. Serotype switching events resulting in more than two descendant isolates are highlighted in red.

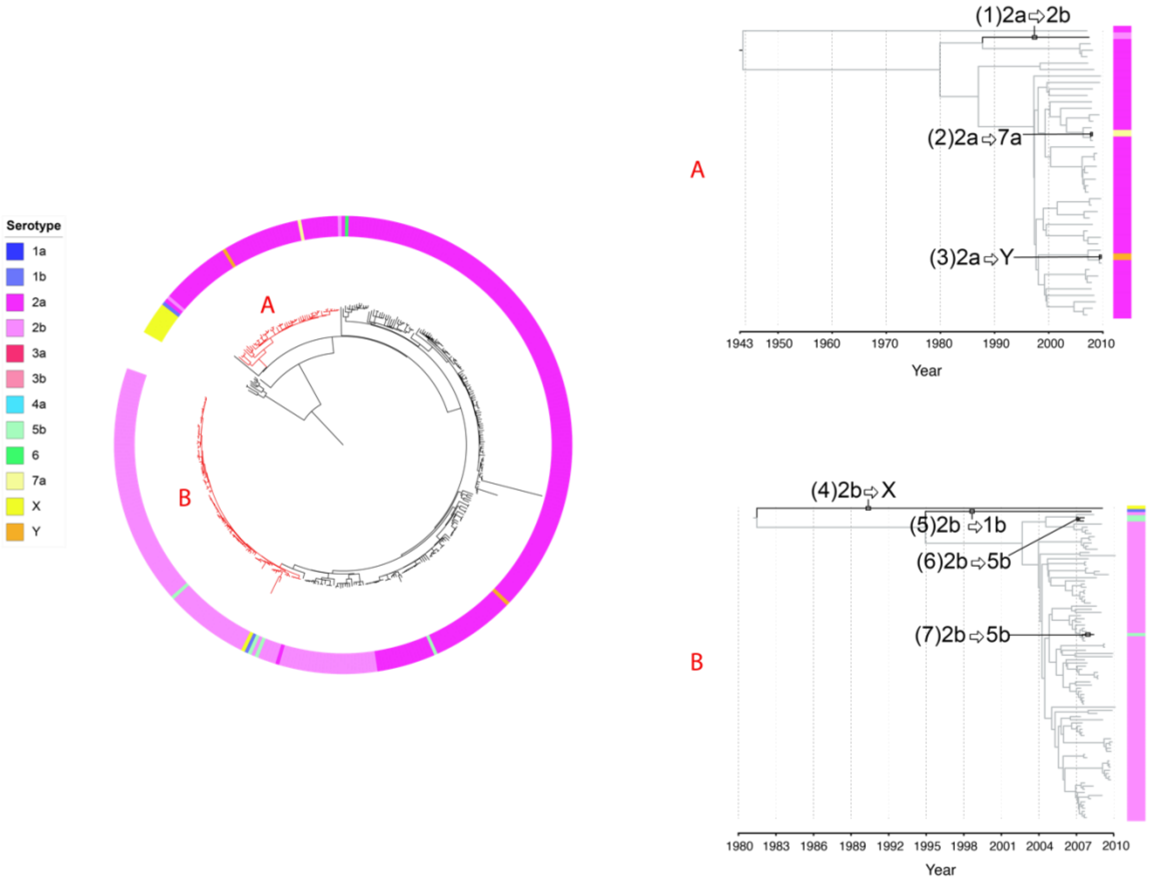

Fig. S8.

Estimation of time frame for serotype switching among *S. flexneri* PG3 isolates. ML phylogenetic tree of *S. flexneri* PG3 (*n*=384) generated using core genome SNPs is displayed on the right. Isolate serotype is displayed on the outer ring, coloured according to the inlaid key displayed next to the tree. Two subclades with branches highlighted in red were selected for BEAST analysis. Maximum clade credibility trees based on two subclades within PG3 are displayed on the left. Independent switching events occurring along the various phylogenetic branches are highlighted in black, labelled and annotated. BEAST estimated time frame of divergence along the branches of the seven isolates that have undergone serotype switching are shown in table S5.

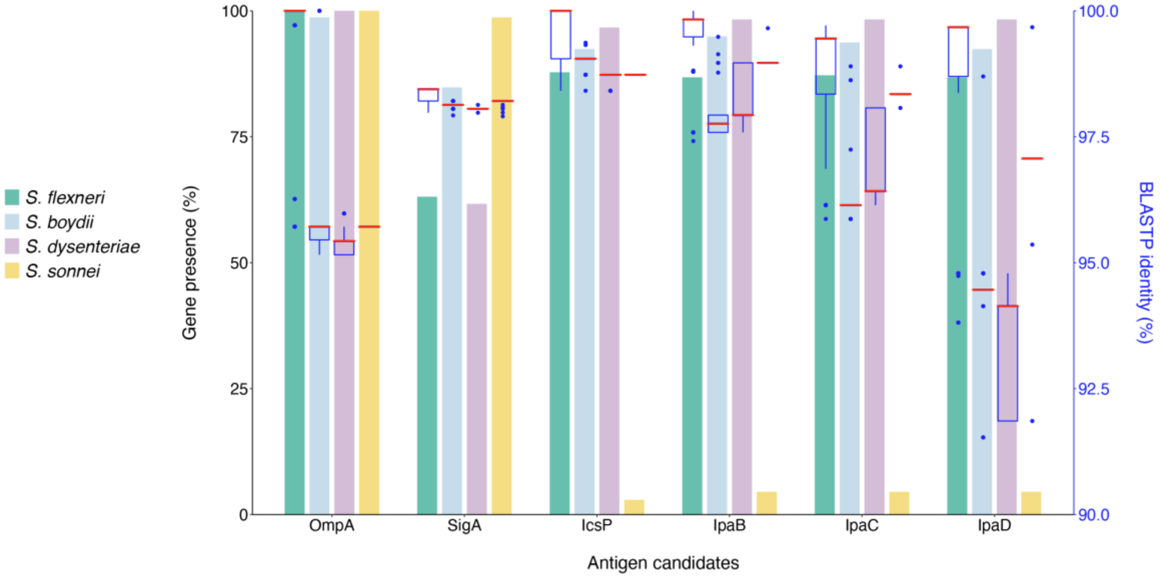

Fig. S9.

The distribution of vaccine antigen candidate and protein sequence identity among *Shigella* spp. (A) Lefthand y-axis refers to the grouped bar plot displaying presence of vaccine candidate genes identified among *Shigella* isolates from GEMS. Bars are grouped by genes and coloured according to species. Righthand y-axis (blue) refers to the boxplot displaying the interquartile range, median (red) and minimum/maximum pairwise percentage identity of the amino acid sequences of antigen vaccine candidates among GEMS, compared against the reference sequences. Presence of genes were identified using BLASTn search against draft genome assemblies and amino acid sequence percentage identity were inferred using BLASTp. (B) Mapping coverage of *Shigella* spp. virulence plasmid. Low percentage of virulence plasmid were detected among *S. sonnei* isolates, likely contributed by the fact that *S. sonnei* virulence plasmid is comparatively unstable and often lost during subculturing.

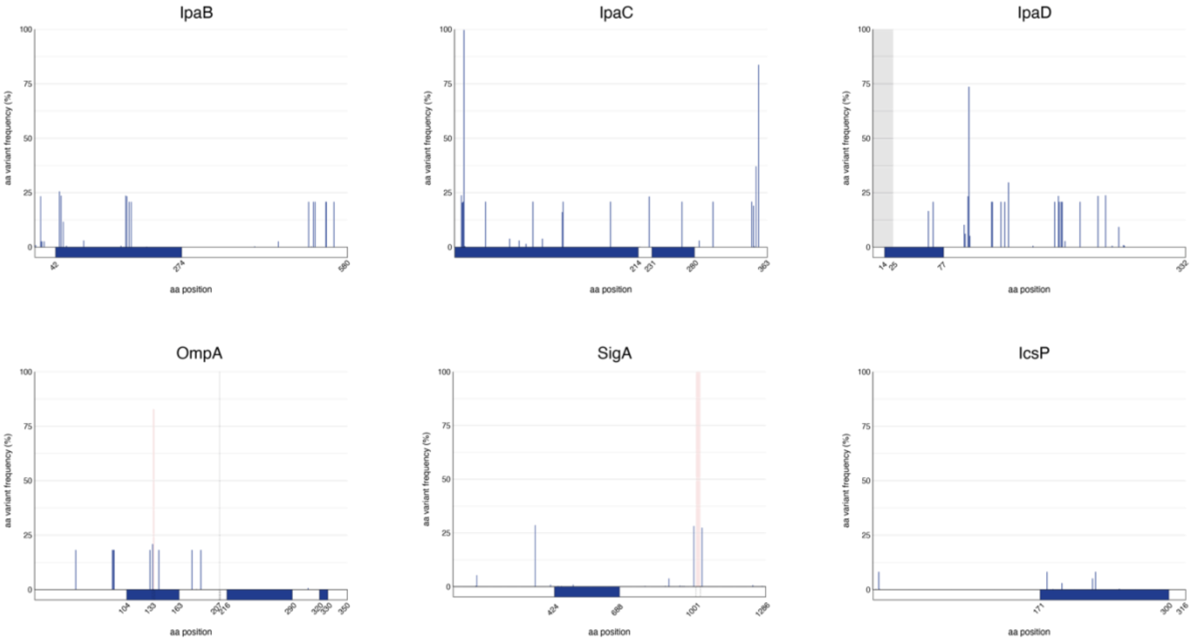

Fig. S10.

Frequency of amino acid variation among *S. flexneri* population for antigen vaccine candidates. Frequency of amino acid variations within *S. flexneri* genomes for the six vaccine candidate protein sequences. For each protein sequence, the proportion of genomes with the variant is shown along the y-axis with the position of the variant plotted along the x-axis. Grey bars highlight regions where there is a deletion and red bars highlight insertions. Schematic of the known epitope positions (in blue) for the protein sequences are displayed below the x-axis.

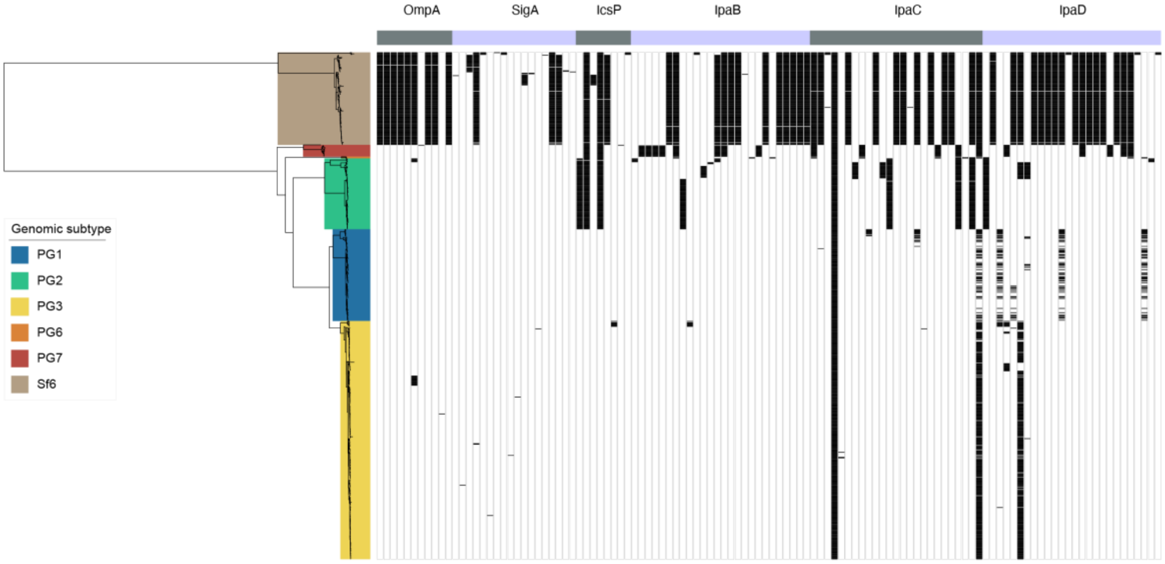

608

609 **Fig. S11.**

610 Vaccine antigen variation among *S. flexneri* subtypes. ML phylogenetic tree of 806 *S. flexneri* isolates based
611 on core genome SNPs is displayed on the left, the six subtypes identified among the population are
612 highlighted in different colours according to the inlaid key. The alternating grey and purple colour blocks
613 displayed above the top panel represents the six antigen vaccine candidates assessed in the current study.
614 The matrix in the centre demonstrates presence (in black) of aa variation for each antigen vaccine. Only
615 variable sites are displayed.

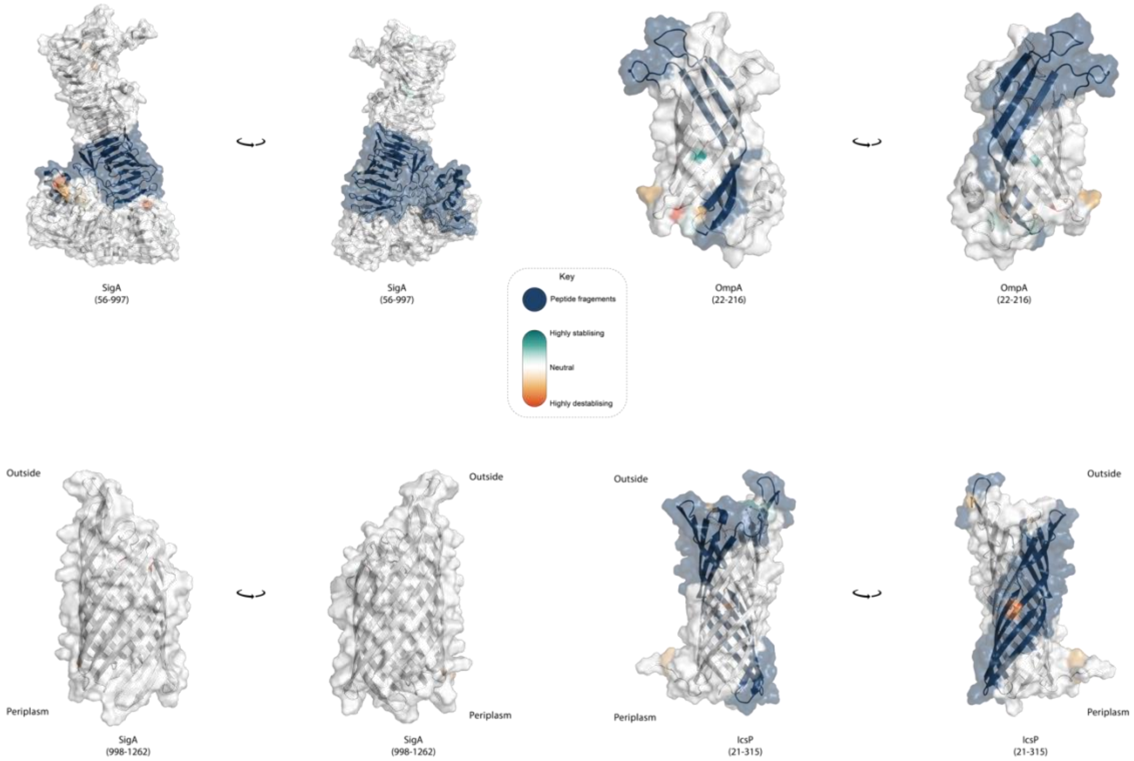

Fig. S12.
Visualization of mutations on modelled SigA, OmpA and IcsP protein antigens. Visualisation of mutations on modelled proteins, with protein residues modelled shown in brackets. Peptide fragments for OmpA, SigA and IcsP that are used for vaccine development are coloured in blue. Predicted effects of mutations within the proteins are coloured using the scale shown in the key. OmpA, SigA and IcsP are orientated so that the extracellular space is located at the top of the figure, and the periplasmic space is at the bottom.

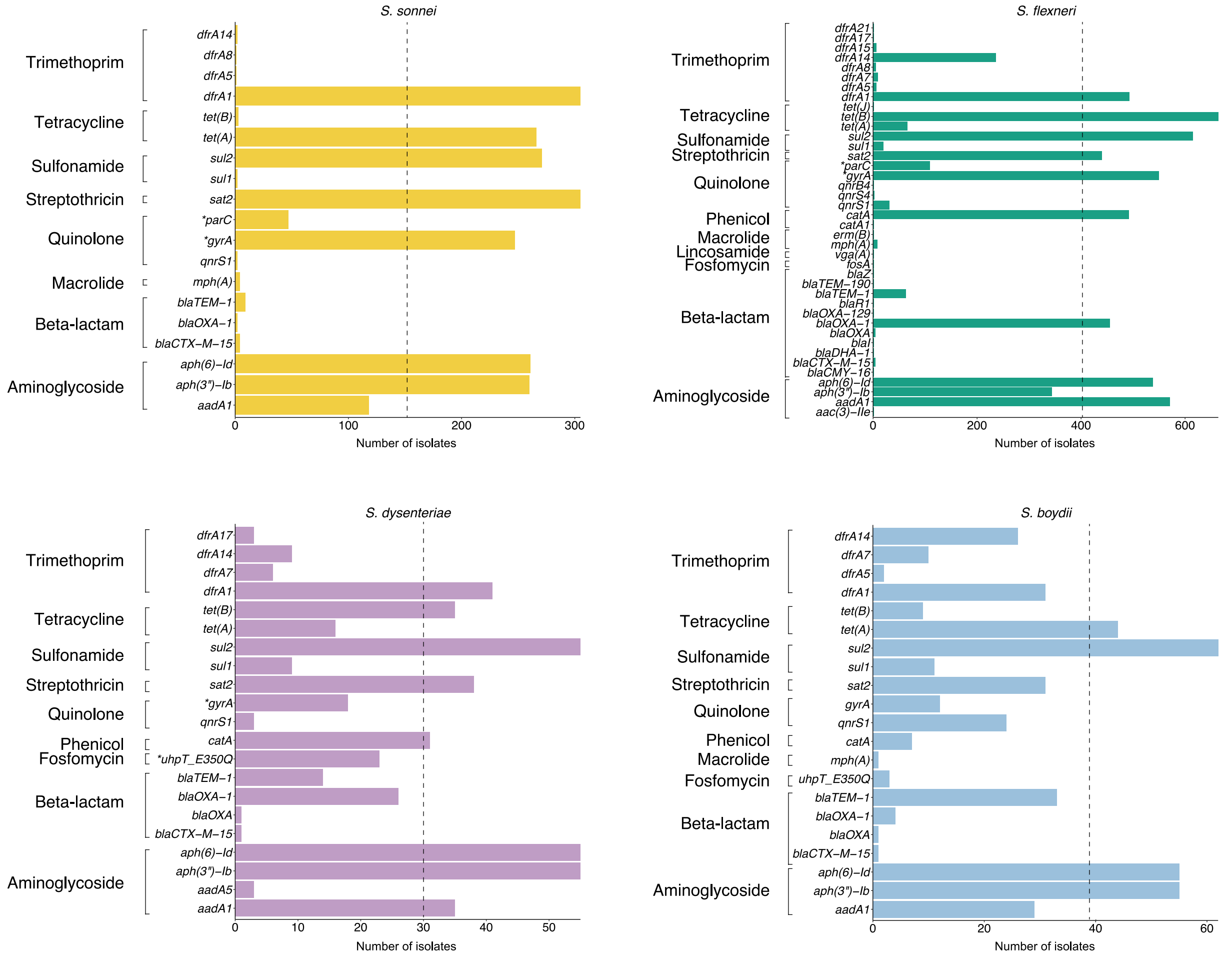

623

624 **Fig. S13.**

625 Prevalence of genetic determinants conferring AMR among *Shigella* spp. Bar plots shows the number of
626 genetic determinants detected in *S. sonnei*, *S. flexneri*, *S. dysenteriae* and *S. boydii* isolates that confer
627 resistance or reduced susceptibility to various antimicrobials. Genes and point mutations (indicated with an
628 asterisk) are plotted along the y-axis and grouped by drug class (displayed on the left). The dashed lines
629 highlight genetic determinants identified in half or more of the isolates for each species.

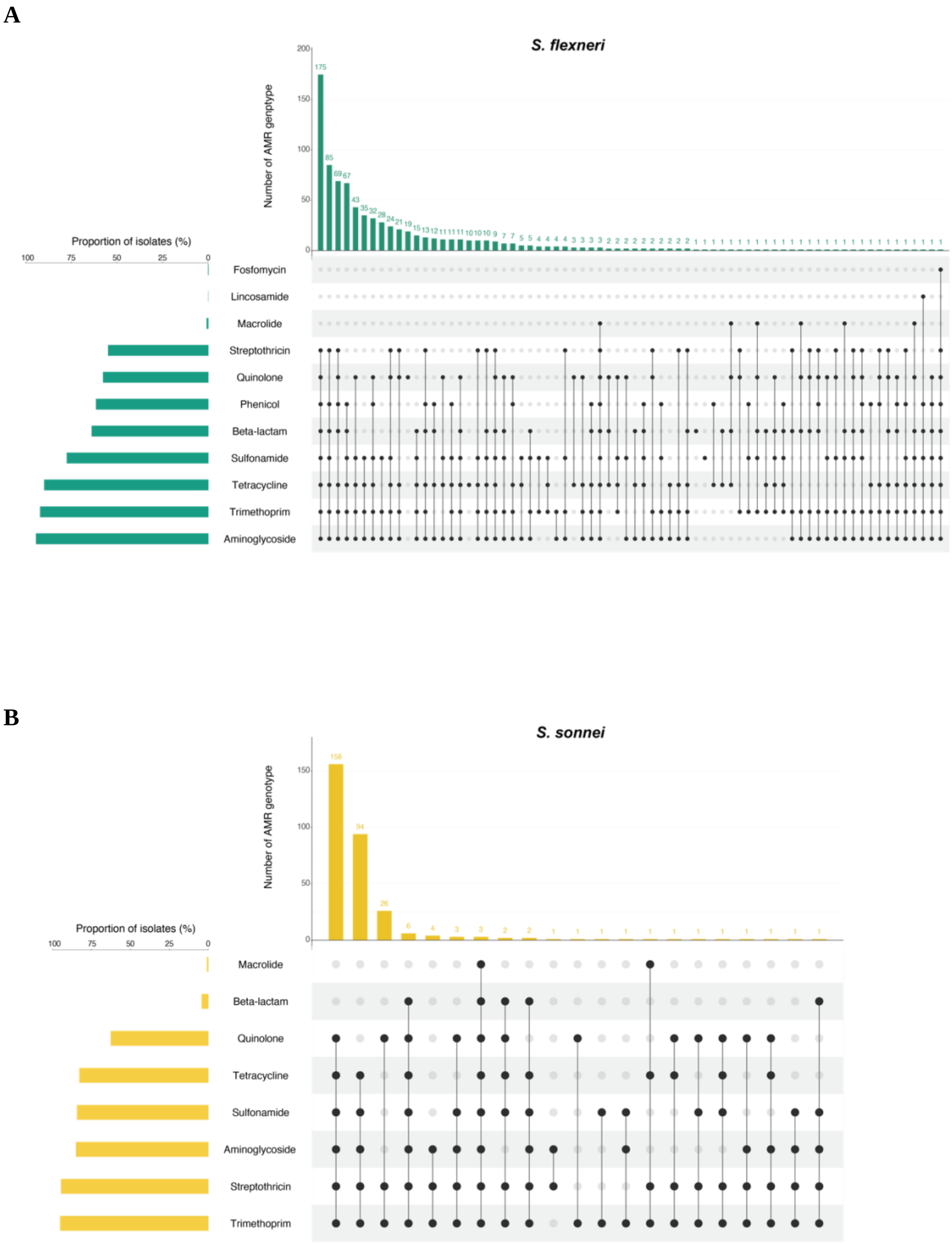
A
S. flexneri
Number of AMR genptype
200
150
100
50
0
175
85
69
67
43
35
32
28
24
21
19
15
13
12
11
11
11
10
10
10
9
7
7
5
5
4
4
4
4
3
3
3
3
2
1
Proportion of isolates (%)
100
75
50
25
0
Fosfomycin
Lincosamide
Macrolide
Streptothricin
Quinolone
Phenicol
Beta-lactam
Sulfonamide
Tetracycline
Trimethoprim
Aminoglycoside
B
S. sonnei
Number of AMR genotype
150
100
50
0
156
94
26
6
4
3
3
2
2
1
Proportion of isolates (%)
100
75
50
25
0
Macrolide
Beta-lactam
Quinolone
Tetracycline
Sulfonamide
Aminoglycoside
Streptothricin
Trimethoprim

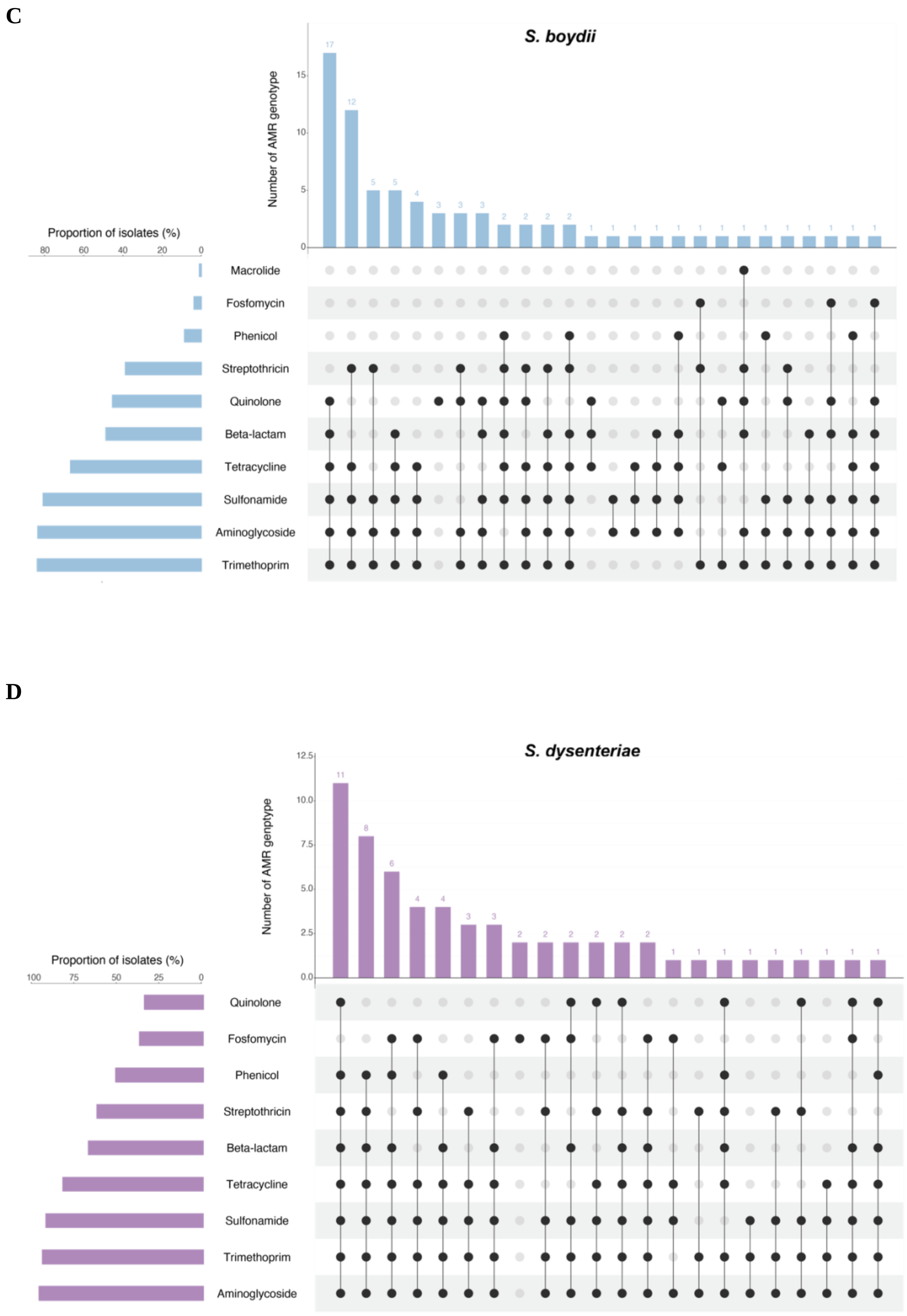
C
S. boydii
Number of AMR genotype
0
5
10
15
17
12
5
5
4
3
3
3
2
2
2
2
1
1
1
1
1
1
1
1
1
1
1
1
1
1
Proportion of isolates (%)
80
60
40
20
0
Macrolide
Fosfomycin
Phenicol
Streptothricin
Quinolone
Beta-lactam
Tetracycline
Sulfonamide
Aminoglycoside
Trimethoprim
D
S. dysenteriae
Number of AMR genptype
0.0
2.5
5.0
7.5
10.0
12.5
11
8
6
4
4
3
3
2
2
2
2
2
2
1
1
1
1
1
1
1
1
1
Proportion of isolates (%)
100
75
50
25
0
Quinolone
Fosfomycin
Phenicol
Streptothricin
Beta-lactam
Tetracycline
Sulfonamide
Trimethoprim
Aminoglycoside

Fig. S14.

Diversity of AMR genotype resistance profiles. UpSet plots illustrate the AMR genotype resistance profiles for (A) *S. flexneri*, (B) *S. sonnei*, (C) *S. boydii* and (D) *S. dysenteriae*. Genotypic AMR profiles are shown in the combination matrix in the center panel. Each column represents a unique genotypic profile, where each black dot represents presence of a genetic determinant conferring resistance or reduced susceptibility to a drug class (displayed on the left). The vertical the bar plot above the matrix displays the number of isolates with a particular profile, with the exact number of isolates displayed above each bar. The horizontal bar plot on the left of the matrix illustrates the proportion of isolates containing AMR genetic determinants associated with a drug class.

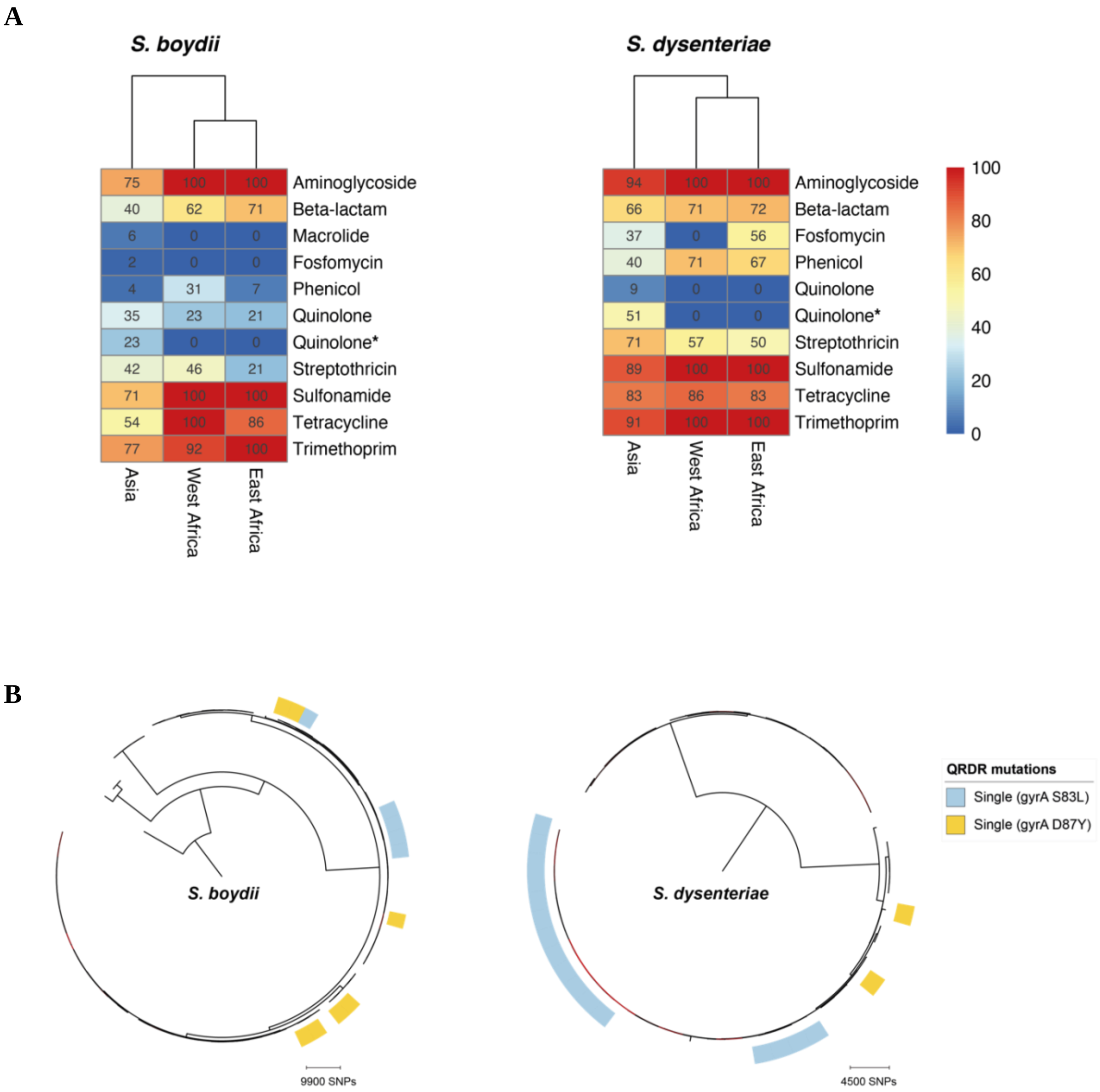

Fig. S15.

Detection of known AMR genetic determinants conferring resistance (reduced susceptibility marked with asterisk) to various drug class, grouped by region (A) and convergent evolution of ciprofloxacin resistance (B) for *S. boydii* and *S. dysenteriae*.

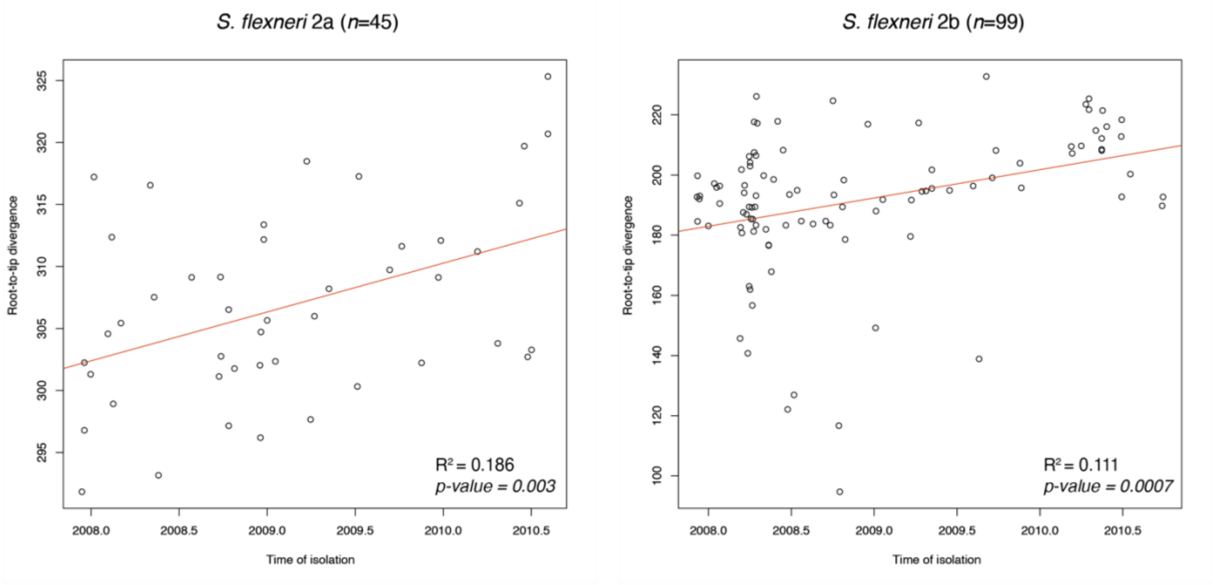

Fig. S16.

Temporal phylogenetic signal for *S. flexneri*. Correlation between isolate sampling time in months (x-axis) and phylogenetic root-to-tip divergence (y-axis), as estimated by TempEst based on ML phylogeny of each subclade. The two datasets correspond to *S. flexneri* 2a isolates belonging to node A (left) and *S. flexneri* 2b isolates belonging to node B (right) from PG3 in fig. S8. The linear regression line is coloured in red, with the coefficient of determination (R^2) and *p*-value displayed for each plot.

Table S1.

Details of *Shigella* isolates used in this study. Includes accession numbers of the sequencing reads used in the study, *Shigella* serotype, assembly statistics, year and country of isolation, condition of the child (case/control) from which the isolate was derived from as defined by GEMS, genomic subtype, AMR genes and QRDR mutations.

See separate Excel file

Table S2.

Details of publicly available *E.coli*/*Shigella* genomes used in this study.

Accession	strain	Species / serotype	Phylogroup/Lineage/subtype
ERR028677	5417_1#4	*S. sonnei*	Central Asia III
ERR028679	5417_1#6	*S. sonnei*	Central Asia III
ERR024610	5008_7#5	*S. sonnei*	Central Asia III
ERR028705	5417_3#8	*S. sonnei*	Central Asia III
ERR024611	5008_7#6	*S. sonnei*	Central Asia III
ERR200544	8403_8#89	*S. sonnei*	V
ERR200550	8403_8#95	*S. sonnei*	V
ERR025737	5236_6#2	*S. sonnei*	IV
ERR025768	5236_8#9	*S. sonnei*	Global III
ERR316396	9803_4#91	*S. sonnei*	Global III
ERR200471	8403_8#16	*S. sonnei*	Global III
ERR025765	5236_8#6	*S. sonnei*	I
ERR025722	5236_5#10	*S. sonnei*	I
ERR024606	5008_7#11	*S. sonnei*	I
ERR025754	5236_7#7	*S. sonnei*	I
ERR025735	5236_6#10	*S. sonnei*	II
ERR025726	5236_5#3	*S. sonnei*	II
ERR028675	5417_1#2	*S. sonnei*	II
ERR028673	5417_1#11	*S. sonnei*	II
ERR025751	5236_7#4	*S. sonnei*	II
ERR025762	5236_8#3	*S. sonnei*	II
ERR025689	5236_1#5	*S. sonnei*	II
ERR025692	5236_1#8	*S. sonnei*	II
ERR025724	5236_5#12	*S. sonnei*	II
ERR028700	5417_3#3	*S. sonnei*	II
ERR028688	5417_2#2	*S. sonnei*	III
ERR025747	5236_7#10	*S. sonnei*	III
ERR025749	5236_7#2	*S. sonnei*	III
ERR025702	5236_2#5	*S. sonnei*	III
ERR025700	5236_2#3	*S. sonnei*	III
ERR025701	5236_2#4	*S. sonnei*	III
ERR025748	5236_7#11	*S. sonnei*	III
ERR028695	5417_2#9	*S. sonnei*	III
ERR025698	5236_2#12	*S. sonnei*	III
ERR316322	9803_4#17	*S. sonnei*	Latin America IIIa
ERR212328	8489_1#60	*S. sonnei*	Latin America IIIa
ERR316241	9789_6#32	*S. sonnei*	Latin America IIIa
ERR025767	5236_8#8	*S. sonnei*	OJCA
ERR190834	8290_4#28	*S. sonnei*	OJCA
ERR319257	9870_7#10	*S. sonnei*	OJCA

NC_007384	Ss046	*S. sonnei*	III
LVIU01000110.1	ASM164910v1	*S. flexneri* 4s	
NZ_CM001474.1	M90T	*S. flexneri* 5a	
NC_004741.1	2457T	*S. flexneri* 2a	
ERR042803	ERR042803	*S. flexneri* 2a	Phylogroup 3
ERR042850	ERR042850	*S. flexneri* 2a	Phylogroup 3
ERR048281	ERR048281	*S. flexneri*	Phylogroup 2
ERR048288	ERR048288	*S. flexneri*	Phylogroup 6
ERR048302	ERR048302	*S. flexneri* 2a	Phylogroup 3
ERR048305	ERR048305	*S. flexneri*	Phylogroup 1
ERR048317	ERR048317	*S. flexneri*	Phylogroup 7
ERR048339	ERR048339	*S. flexneri* 2a	Phylogroup 3
ERR126987	ERR126987	*S. flexneri* 2a	Phylogroup 3
ERR126993	ERR126993	*S. flexneri*	Phylogroup 2
ERR127032	ERR127032	*S. flexneri* 1a	PHE type strain
ERR127033	ERR127033	*S. flexneri* 1b	PHE type strain
ERR127034	ERR127034	*S. flexneri* 1c	PHE type strain
ERR127035	ERR127035	*S. flexneri* 2a	PHE type strain
ERR127036	ERR127036	*S. flexneri* 2b	PHE type strain
ERR127037	ERR127037	*S. flexneri* 3a	PHE type strain
ERR127038	ERR127038	*S. flexneri* 3b	PHE type strain
ERR127039	ERR127039	*S. flexneri* 3c	PHE type strain
ERR127040	ERR127040	*S. flexneri* 4a	PHE type strain
ERR127041	ERR127041	*S. flexneri* 4b	PHE type strain
ERR127043	ERR127043	*S. flexneri* 5a	PHE type strain
ERR127044	ERR127044	*S. flexneri* 5b	PHE type strain
ERR127046	ERR127046	*S. flexneri*	Phylogroup 4
ERR127047	ERR127047	*S. flexneri* Y	PHE type strain
ERR127048	ERR127048	*S. flexneri* E1037	PHE type strain
ERR1363976	ERR1363976	*S. flexneri* 2a	Phylogroup 3 Central Asia
ERR1364007	ERR1364007	*S. flexneri* 2a	Phylogroup 3 Central Asia
ERR1364014	ERR1364014	*S. flexneri* 2a	Phylogroup 3 Minor MSM clade
ERR1364050	ERR1364050	*S. flexneri* 2a	Phylogroup 3 Minor MSM clade
ERR1364087	ERR1364087	*S. flexneri* 2a	Phylogroup 3 Central Asia
ERR1364097	ERR1364097	*S. flexneri* 2a	Phylogroup 1 Central Asia
ERR1364106	ERR1364106	*S. flexneri* 2a	Phylogroup 3 Major MSM clade
ERR1364137	ERR1364137	*S. flexneri* 2a	Phylogroup 3 Major MSM clade
ERR200376	ERR200376	*S. flexneri* 2a	Phylogroup 3
ERR217085	ERR217085	*S. flexneri*	Phylogroup 1

ERR449043	ERR449043	*S. flexneri* 3a	MSM-outbreak associated
ERR449077	ERR449077	*S. flexneri* 3a	MSM-outbreak associated
ERR559526	ERR559526	*S. flexneri* 2a	NCTC1
ERR832464	ERR832464	*S. flexneri*	Phylogroup 5
ERR832481	ERR832481	*S. flexneri*	Phylogroup 3
SRR7886341	SRR7886341	*S. flexneri*	MSM associated
NC_017328.1	ASM2224v1	*S. flexneri*	
NC_004337	S. flexneri 2a str. 301	*S. flexneri 2a*	Phylogroup 3
NC_007606	*S. dysenteriae* Sd197	*S. dysenteriae*	
ERR1013692	ERR1013692	*S. dysenteriae* type 1	IV
ERR1013770	ERR1013770	*S. dysenteriae* type 1	IIIa
ERR1014006	ERR1014006	*S. dysenteriae* type 1	IIId
ERR1014139	ERR1014139	*S. dysenteriae* type 1	IIIc
ERR1014187	ERR1014187	*S. dysenteriae* type 1	IV
ERR1014220	ERR1014220	*S. dysenteriae* type 1	II
ERR1014530	ERR1014530	*S. dysenteriae* type 1	IIIc
ERR1014532	ERR1014532	*S. dysenteriae* type 1	IIId
ERR1014536	ERR1014536	*S. dysenteriae* type 1	I
ERR1014541	ERR1014541	*S. dysenteriae* type 1	II
ERR1014551	ERR1014551	*S. dysenteriae* type 1	IIIb
ERR279284	ERR279284	*S. dysenteriae* type 1	II
GCA_000268105	SD_225-75	*S. dysenteriae* type 2	S1
GCF_000815495	SD_S6205	*S. dysenteriae* type 2	S3
ERR200454	SB_K-11124	*S. boydii* (ST 1767)	
NZ_AMKG01000009	248-1B	*S. boydii*	3
NC_010658	3083-94	*S. boydii*	2
AMJZ00000000	SB_08_0009	*S. boydii*	3
AMKA00000000	SB_08_0280	*S. boydii*	2

AMKB00000000	SB_08_2671	*S. boydii*	3
AMKC00000000	SB_08_2675	*S. boydii*	2
AMKD00000000	SB_08_6341	*S. boydii*	2
AMKE00000000	SB_09_0344	*S. boydii*	2
AFGC00000000	SB_3594-74	*S. boydii*	3
AKNB00000000	SB_4444-74	*S. boydii*	3
AFGE00000000	SB_5216-82	*S. boydii*	1
AKNA00000000	SB_965-58	*S. boydii*	1
AMJX00000000	SB_S7334	*S. boydii*	3
NC_010658	3083-94	*S. boydii*	
AAJT00000000	B7A	*E. coli*	
AM946981	BL21(DE3)	*E. coli* O7	
NC_009801	E24377A	*E. coli* O139:H28	
SRR2169557	IAI1-117	*E. coli* O8	
SRR306102	K12-W3110	*E. coli* O16	
NC_011751	UMN026	*E. coli* O17:K52:H18	
NC_013941	CB9615	*E. coli* O55:H7	

Table S3.

Association of *S. flexneri* genomic subtype / serotype with case status.

Genomic subtype / serotype	OR	95% CI	z statistic	p-value
Sf6	0.5043	0.3198 - 0.7953	2.945	0.0032
PG1	0.5773	0.3619 - 0.9211	2.305	0.0212
PG2	0.8926	0.5102 - 1.5616	0.398	0.6906
PG3	2.3196	1.5051 - 3.5748	3.813	0.0001
PG6	1.1339	0.0582 - 22.1005	0.083	0.9339
PG7	2.9426	0.3889 - 22.2638	1.045	0.2959
1a	0.8088	0.0386 - 16.9574	0.137	0.8913
1b	0.6867	0.3942 - 1.1961	1.328	0.1843
2a	1.9329	1.1712 - 3.1900	2.578	0.0099
2b	2.2614	1.1117 - 4.5997	2.252	0.0243
3a	0.8926	0.5102 - 1.5616	0.398	0.6906
4a	0.7946	0.3230 - 1.9548	0.501	0.6167
5b	0.4798	0.0495 - 4.6540	0.633	0.5264
6	0.4829	0.3072 - 0.7590	3.155	0.0016
7a	0.6029	0.2399 - 1.5151	1.076	0.2818
Y	1.46	0.0781 - 27.3032	0.253	0.8001
X	1.6157	0.2048 - 12.7458	0.455	0.6489

Table S4.

Details of serotype determining genes facilitating *S. flexneri* (*n*=72) serotype switching.

See separate Excel file

Table S5.

BEAST estimated timeframe for serotype switching among *S. flexneri* PG3 isolates.

Switch ID[#]	**Subclade**[¶]	**Serotype change**	**Molecular serotype gene detected**[&]	**Median branch length (days)**[$]	**95% HPD branch length (days)**
3	A	2a → Y	-	159	16 - 344
2	A	2a → 7a	*gtrII*	154	27 - 307
1	A	2a → 2b	*gtrII, gtrX*	7203	4792 - 10009
7	B	2b → 5b	*gtrII, gtrX*	348	244 - 479
6	B	2b → 5b	*gtrII, gtrX*	254	134 - 491
5	B	2b → 1b	*gtrI, gtrII, Oac1b*	4888	2962 - 7114
4	B	2b → X	*gtrX, gtrll*	10206	5494 - 15408

Footnotes:

[#] Serotype switching event labelled according to Fig S8

[¶] Phylogenetic subclade isolate belong to

[&] Presence of serotype determining genes, as detected by ShigaTyper, - indicates no genes were detected.

[$] Phylogenetic branch length represents divergence time, predicted by BEAST and inferred from a time-scaled tree.

Table S6.

An overview of the protein modelling. Table includes information about the antigen candidates modelled, the range of residues the proteins were modelled over, homologues used in template modelling and the QMEAN method and score.

Species	Antigen candidates	Phylogroup	Serotype	Start	Finish	Homolog	Sequence Identity	QMEAN method	Average local QMEAN score
S. flexneri	OmpA	PG3	5A	22	216	1QJP	93%	QMEANDisCo	0.46
S. flexneri	OmpA	PG3	5A	349	490	1R1M	41%	QMEANDisCo	0.31
S. flexneri	SigA	PG3	2A	56	997	3SZE	44%	QMEANDisCo	0.71
S. flexneri	SigA	PG3	2A	998	1262	2QOM	85%	QMEANDisCo	0.83
S. flexneri	IcsP	PG3	5A	21	315	1I78	60%	QMEANDisCo	0.81
S. flexneri	IpaB	PG3	5A	1	222	3U0C	76%	QMEANBrane	0.83
S. flexneri	IpaB	PG3	5A	223	553	3WXX	19%	QMEANBrane	0.79
S. flexneri	IpaC	PG3	5A	1	363	-	-	QMEANBrane	0.85
S. flexneri	IpaD	PG3	5A	1	332	3R9V	100%	QMEANBrane	0.80

Table S7.

Details of amino acid variants identified for the six antigen candidates among *S. flexneri* isolates from GEMS. Table includes variant type, variant location, reference and alternative variant, and energy score of the variant as predicted by premPS.

See separate Excel file

Reference

1. Khalil IA, Troeger C, Blacker BF, Rao PC, Brown A, Atherly DE, et al. Morbidity and mortality due to shigella and enterotoxigenic Escherichia coli diarrhoea: the Global Burden of Disease Study 1990-2016. The Lancet infectious diseases. 2018;18(11):1229-40.
2. Kotloff KL, Nataro JP, Blackwelder WC, Nasrin D, Farag TH, Panchalingam S, et al. Burden and aetiology of diarrhoeal disease in infants and young children in developing countries (the Global Enteric Multicenter Study, GEMS): a prospective, case-control study. Lancet. 2013;382(9888):209-22.
3. Liu J, Platts-Mills JA, Juma J, Kabir F, Nkeze J, Okoi C, et al. Use of quantitative molecular diagnostic methods to identify causes of diarrhoea in children: a reanalysis of the GEMS case-control study. Lancet. 2016;388(10051):1291-301.
4. Kotloff KL, Riddle MS, Platts-Mills JA, Pavlinac P, Zaidi AKM. Shigellosis. Lancet. 2018;391(10122):801-12.
5. Shrivastava SR, Shrivastava PS, Ramasamy J. World health organization releases global priority list of antibiotic-resistant bacteria to guide research, discovery, and development of new antibiotics. Journal of Medical Society. 2018;32(1):76.
6. Barry EM, Pasetti MF, Sztein MB, Fasano A, Kotloff KL, Levine MM. Progress and pitfalls in Shigella vaccine research. Nat Rev Gastroenterol Hepatol. 2013;10(4):245-55.
7. Cohen D, Green MS, Block C, Slepon R, Ofek I. Prospective study of the association between serum antibodies to lipopolysaccharide O antigen and the attack rate of shigellosis. Journal of clinical microbiology. 1991;29(2):386-9.
8. Ferreccio C, Prado V, Ojeda A, Cayyazo M, Abrego P, Guers L, et al. Epidemiologic patterns of acute diarrhea and endemic Shigella infections in children in a poor periurban setting in Santiago, Chile. Am J Epidemiol. 1991;134(6):614-27.
9. Formal SB, Oaks EV, Olsen RE, Wingfield-Eggleston M, Snoy PJ, Cogan JP. Effect of prior infection with virulent Shigella flexneri 2a on the resistance of monkeys to subsequent infection with Shigella sonnei. J Infect Dis. 1991;164(3):533-7.
10. Kotloff KL, Nataro JP, Losonsky GA, Wasserman SS, Hale TL, Taylor DN, et al. A modified Shigella volunteer challenge model in which the inoculum is administered with bicarbonate buffer: clinical experience and implications for Shigella infectivity. Vaccine. 1995;13(16):1488-94.
11. Levine MM, Kotloff KL, Barry EM, Pasetti MF, Sztein MB. Clinical trials of Shigella vaccines: two steps forward and one step back on a long, hard road. Nat Rev Microbiol. 2007;5(7):540-53.
12. Ashkenazi S, Cohen D. An update on vaccines against Shigella. Ther Adv Vaccines. 2013;1(3):113-23.
13. Talaat KR, Alaimo C, Martin P, Bourgeois AL, Dreyer AM, Kaminski RW, et al. Human challenge study with a Shigella bioconjugate vaccine: Analyses of clinical efficacy and correlate of protection. EBioMedicine. 2021;66:103310.
14. Passwell JH, Ashkenazi S, Banet-Levi Y, Ramon-Saraf R, Farzam N, Lerner-Geva L, et al. Age-related efficacy of Shigella O-specific polysaccharide conjugates in 1-4-year-old Israeli children. Vaccine. 2010;28(10):2231-5.
15. Turbyfill KR, Kaminski RW, Oaks EV. Immunogenicity and efficacy of highly purified invasin complex vaccine from Shigella flexneri 2a. Vaccine. 2008;26(10):1353-64.

16. Martinez-Becerra FJ, Kissmann JM, Diaz-McNair J, Choudhari SP, Quick AM, Mellado-Sanchez G, et al. Broadly protective Shigella vaccine based on type III secretion apparatus proteins. Infect Immun. 2012;80(3):1222-31.

17. Davies MR, McIntyre L, Mutreja A, Lacey JA, Lees JA, Towers RJ, et al. Atlas of group A streptococcal vaccine candidates compiled using large-scale comparative genomics. Nat Genet. 2019;51(6):1035-43.

18. Telford JL. Bacterial genome variability and its impact on vaccine design. Cell Host Microbe. 2008;3(6):408-16.

19. Livio S, Strockbine NA, Panchalingam S, Tennant SM, Barry EM, Marohn ME, et al. Shigella isolates from the global enteric multicenter study inform vaccine development. Clin Infect Dis. 2014;59(7):933-41.

20. Connor TR, Barker CR, Baker KS, Weill FX, Talukder KA, Smith AM, et al. Species-wide whole genome sequencing reveals historical global spread and recent local persistence in Shigella flexneri. Elife. 2015;4:e07335.

21. Holt KE, Baker S, Weill FX, Holmes EC, Kitchen A, Yu J, et al. Shigella sonnei genome sequencing and phylogenetic analysis indicate recent global dissemination from Europe. Nat Genet. 2012;44(9):1056-9.

22. Njamkepo E, Fawal N, Tran-Dien A, Hawkey J, Strockbine N, Jenkins C, et al. Global phylogeography and evolutionary history of Shigella dysenteriae type 1. Nat Microbiol. 2016;1:16027.

23. Kania DA, Hazen TH, Hossain A, Nataro JP, Rasko DA. Genome diversity of Shigella boydii. Pathog Dis. 2016;74(4):ftw027.

24. Hawkey J, Paranagama K, Baker KS, Bengtsson RJ, Weill F-X, Thomson NR, et al. Global population structure and genotyping framework for genomic surveillance of the major dysentery pathogen, Shigella sonnei. Nature Communications. 2021;12(1):2684.

25. Sahl JW, Morris CR, Emberger J, Fraser CM, Ochieng JB, Juma J, et al. Defining the phylogenomics of Shigella species: a pathway to diagnostics. J Clin Microbiol. 2015;53(3):951-60.

26. von Seidlein L, Kim DR, Ali M, Lee H, Wang X, Thiem VD, et al. A multicentre study of Shigella diarrhoea in six Asian countries: disease burden, clinical manifestations, and microbiology. PLoS Med. 2006;3(9):e353.

27. Ye C, Lan R, Xia S, Zhang J, Sun Q, Zhang S, et al. Emergence of a new multidrug-resistant serotype X variant in an epidemic clone of Shigella flexneri. J Clin Microbiol. 2010;48(2):419-26.

28. Allison GE, Verma NK. Serotype-converting bacteriophages and O-antigen modification in Shigella flexneri. Trends Microbiol. 2000;8(1):17-23.

29. Sun Q, Knirel YA, Lan R, Wang J, Senchenkova SN, Jin D, et al. A novel plasmid-encoded serotype conversion mechanism through addition of phosphoethanolamine to the O-antigen of Shigella flexneri. PLoS One. 2012;7(9):e46095.

30. Weinberger DM, Malley R, Lipsitch M. Serotype replacement in disease after pneumococcal vaccination. Lancet. 2011;378(9807):1962-73.

31. Brueggemann AB, Pai R, Crook DW, Beall B. Vaccine escape recombinants emerge after pneumococcal vaccination in the United States. PLoS Pathog. 2007;3(11):e168.

32. McVicker G, Tang CM. Deletion of toxin-antitoxin systems in the evolution of Shigella sonnei as a host-adapted pathogen. Nat Microbiol. 2016;2:16204.

33. Garcia-Beltran WF, Lam EC, St Denis K, Nitido AD, Garcia ZH, Hauser BM, et al. Multiple SARS-CoV-2 variants escape neutralization by vaccine-induced humoral immunity. Cell. 2021.

34. Zhou D, Dejnirattisai W, Supasa P, Liu C, Mentzer AJ, Ginn HM, et al. Evidence of escape of SARS-CoV-2 variant B.1.351 from natural and vaccine-induced sera. Cell. 2021.

35. Mills JA, Buysse JM, Oaks EV. Shigella flexneri invasion plasmid antigens B and C: epitope location and characterization with monoclonal antibodies. Infect Immun. 1988;56(11):2933-41.

36. Turbyfill KR, Mertz JA, Mallett CP, Oaks EV. Identification of epitope and surface-exposed domains of Shigella flexneri invasion plasmid antigen D (IpaD). Infect Immun. 1998;66(5):1999-2006.

37. Czerkinsky C, Kim DW. Shigella protein antigens and methods. US Patent 8168203; 2012.

38. Pore D, Mahata N, Pal A, Chakrabarti MK. Outer membrane protein A (OmpA) of Shigella flexneri 2a, induces protective immune response in a mouse model. PLoS One. 2011;6(7):e22663.

39. Organization WH. Guidelines for the control of shigellosis, including epidemics due to Shigella dysenteriae type 1. 2005.

40. Chung The H, Baker S. Out of Asia: the independent rise and global spread of fluoroquinolone-resistant Shigella. Microb Genom. 2018;4(4).

41. Sadouki Z, Day MR, Doumith M, Chattaway MA, Dallman TJ, Hopkins KL, et al. Comparison of phenotypic and WGS-derived antimicrobial resistance profiles of Shigella sonnei isolated from cases of diarrhoeal disease in England and Wales, 2015. J Antimicrob Chemother. 2017;72(9):2496-502.

42. Baker KS, Dallman TJ, Ashton PM, Day M, Hughes G, Crook PD, et al. Intercontinental dissemination of azithromycin-resistant shigellosis through sexual transmission: a cross-sectional study. Lancet Infect Dis. 2015;15(8):913-21.

43. Williams PCM, Berkley JA. Guidelines for the treatment of dysentery (shigellosis): a systematic review of the evidence. Paediatr Int Child Health. 2018;38(sup1):S50-S65.

44. Chung The H, Rabaa MA, Pham Thanh D, De Lappe N, Cormican M, Valcanis M, et al. South Asia as a Reservoir for the Global Spread of Ciprofloxacin-Resistant Shigella sonnei: A Cross-Sectional Study. PLoS Med. 2016;13(8):e1002055.

45. Chung The H, Boinett C, Pham Thanh D, Jenkins C, Weill FX, Howden BP, et al. Dissecting the molecular evolution of fluoroquinolone-resistant Shigella sonnei. Nat Commun. 2019;10(1):4828.

46. Ingle DJ, Levine MM, Kotloff KL, Holt KE, Robins-Browne RM. Dynamics of antimicrobial resistance in intestinal Escherichia coli from children in community settings in South Asia and sub-Saharan Africa. Nat Microbiol. 2018;3(9):1063-73.

47. Makoni M. Africa's $100-million Pathogen Genomics Initiative. The Lancet Microbe. 2020;1(8):e318.

48. AMR NGHRUoGSo. Whole-genome sequencing as part of national and international surveillance programmes for antimicrobial resistance: a roadmap. BMJ Global Health. 2020;5(11):e002244.

49. Perez-Sepulveda BM, Heavens D, Pulford CV, Predeus AV, Low R, Webster H, et al. An accessible, efficient and global approach for the large-scale sequencing of bacterial genomes. BioRxiv. 2020.

50. Bolger AM, Lohse M, Usadel B. Trimmomatic: a flexible trimmer for Illumina sequence data. Bioinformatics. 2014;30(15):2114-20.

51. Ewels P, Magnusson M, Lundin S, Kaller M. MultiQC: summarize analysis results for multiple tools and samples in a single report. Bioinformatics. 2016;32(19):3047-8.

52. Li H. Aligning sequence reads, clone sequences and assembly contigs with BWA-MEM. arXiv preprint arXiv:13033997. 2013.

53. Li H, Handsaker B, Wysoker A, Fennell T, Ruan J, Homer N, et al. The Sequence Alignment/Map format and SAMtools. Bioinformatics. 2009;25(16):2078-9.

54. Garcia-Alcalde F, Okonechnikov K, Carbonell J, Cruz LM, Gotz S, Tarazona S, et al. Qualimap: evaluating next-generation sequencing alignment data. Bioinformatics. 2012;28(20):2678-9.

55. Arndt D, Grant JR, Marcu A, Sajed T, Pon A, Liang Y, et al. PHASTER: a better, faster version of the PHAST phage search tool. Nucleic Acids Res. 2016;44(W1):W16-21.

56. Quinlan AR. BEDTools: The Swiss-Army Tool for Genome Feature Analysis. Curr Protoc Bioinformatics. 2014;47:11 2 1-34.

57. Croucher NJ, Page AJ, Connor TR, Delaney AJ, Keane JA, Bentley SD, et al. Rapid phylogenetic analysis of large samples of recombinant bacterial whole genome sequences using Gubbins. Nucleic Acids Res. 2015;43(3):e15.

58. Nguyen LT, Schmidt HA, von Haeseler A, Minh BQ. IQ-TREE: a fast and effective stochastic algorithm for estimating maximum-likelihood phylogenies. Mol Biol Evol. 2015;32(1):268-74.

59. Letunic I, Bork P. Interactive Tree Of Life (iTOL) v4: recent updates and new developments. Nucleic Acids Res. 2019;47(W1):W256-W9.

60. Rambaut A, Lam TT, Max Carvalho L, Pybus OG. Exploring the temporal structure of heterochronous sequences using TempEst (formerly Path-O-Gen). Virus Evol. 2016;2(1):vew007.

61. Bouckaert R, Heled J, Kuhnert D, Vaughan T, Wu CH, Xie D, et al. BEAST 2: a software platform for Bayesian evolutionary analysis. PLoS Comput Biol. 2014;10(4):e1003537.

62. Bouckaert RR, Drummond AJ. bModelTest: Bayesian phylogenetic site model averaging and model comparison. BMC Evol Biol. 2017;17(1):42.

63. Rambaut A, Drummond AJ, Xie D, Baele G, Suchard MA. Posterior Summarization in Bayesian Phylogenetics Using Tracer 1.7. Syst Biol. 2018;67(5):901-4.

64. Bouckaert R, Vaughan TG, Barido-Sottani J, Duchene S, Fourment M, Gavryushkina A, et al. BEAST 2.5: An advanced software platform for Bayesian evolutionary analysis. PLoS Comput Biol. 2019;15(4):e1006650.

65. Wick RR, Judd LM, Gorrie CL, Holt KE. Unicycler: resolving bacterial genome assemblies from short and long sequencing reads. PLoS computational biology. 2017;13(6):e1005595.

66. Gurevich A, Saveliev V, Vyahhi N, Tesler G. QUAST: quality assessment tool for genome assemblies. Bioinformatics. 2013;29(8):1072-5.

67. Seemann T. Prokka: rapid prokaryotic genome annotation. Bioinformatics. 2014;30(14):2068-9.

68. Page AJ, Cummins CA, Hunt M, Wong VK, Reuter S, Holden MT, et al. Roary: rapid large-scale prokaryote pan genome analysis. Bioinformatics. 2015;31(22):3691-3.

69. Wu Y, Lau HK, Lee T, Lau DK, Payne J. In Silico Serotyping Based on Whole-Genome Sequencing Improves the Accuracy of Shigella Identification. Appl Environ Microbiol. 2019;85(7).

70. Inouye M, Dashnow H, Raven LA, Schultz MB, Pope BJ, Tomita T, et al. SRST2: Rapid genomic surveillance for public health and hospital microbiology labs. Genome Med. 2014;6(11):90.

71. Altschul SF, Madden TL, Schaffer AA, Zhang J, Zhang Z, Miller W, et al. Gapped BLAST and PSI-BLAST: a new generation of protein database search programs. Nucleic Acids Res. 1997;25(17):3389-402.

72. Larsson A. AliView: a fast and lightweight alignment viewer and editor for large datasets. Bioinformatics. 2014;30(22):3276-8.

73. Hildebrand A, Remmert M, Biegert A, Soding J. Fast and accurate automatic structure prediction with HHpred. Proteins. 2009;77 Suppl 9:128-32.

74. Zimmermann L, Stephens A, Nam SZ, Rau D, Kubler J, Lozajic M, et al. A Completely Reimplemented MPI Bioinformatics Toolkit with a New HHpred Server at its Core. J Mol Biol. 2018;430(15):2237-43.

75. Song Y, DiMaio F, Wang RY, Kim D, Miles C, Brunette T, et al. High-resolution comparative modeling with RosettaCM. Structure. 2013;21(10):1735-42.

76. Yang J, Anishchenko I, Park H, Peng Z, Ovchinnikov S, Baker D. Improved protein structure prediction using predicted interresidue orientations. Proceedings of the National Academy of Sciences. 2020;117(3):1496-503.

77. Studer G, Rempfer C, Waterhouse AM, Gumienny R, Haas J, Schwede T. QMEANDisCo-distance constraints applied on model quality estimation. Bioinformatics. 2020;36(8):2647.

78. Studer G, Biasini M, Schwede T. Assessing the local structural quality of transmembrane protein models using statistical potentials (QMEANBrane). Bioinformatics. 2014;30(17):i505-11.

79. Chen Y, Lu H, Zhang N, Zhu Z, Wang S, Li M. PremPS: Predicting the impact of missense mutations on protein stability. PLoS Comput Biol. 2020;16(12):e1008543.

80. Feldgarden M, Brover V, Haft DH, Prasad AB, Slotta DJ, Tolstoy I, et al. Validating the AMRFinder Tool and Resistance Gene Database by Using Antimicrobial Resistance Genotype-Phenotype Correlations in a Collection of Isolates. Antimicrob Agents Chemother. 2019;63(11).

81. Conway JR, Lex A, Gehlenborg N. UpSetR: an R package for the visualization of intersecting sets and their properties. Bioinformatics. 2017;33(18):2938-40.

82. Hudzicki J. Kirby-Bauer disk diffusion susceptibility test protocol. 2009.